

Abscisic acid employs NRP-dependent PIN2 vacuolar degradation to suppress auxin-mediated primary root elongation in *Arabidopsis*

Yanying Wu¹ , Yue Chang¹, Liming Luo², Wenqi Tian¹, Qingqiu Gong²  and Xinqi Liu¹ 

¹State Key Laboratory of Medicinal Chemical Biology, Tianjin Key Laboratory of Protein Science, College of Life Sciences, Nankai University, Tianjin 300071, China; ²State Key Laboratory of Microbial Metabolism & Joint International Research Laboratory of Metabolic and Developmental Sciences, School of Life Sciences and Biotechnology, Shanghai Jiao Tong University, Shanghai 200240, China

Authors for correspondence:
Qingqiu Gong
Email: gongqingqiu@sjtu.edu.cn

Xinqi Liu
Email: liu2008@nankai.edu.cn

Received: 11 August 2021
Accepted: 25 September 2021

New Phytologist (2021)
doi: 10.1111/nph.17783

Key words: abscisic acid (ABA), *Arabidopsis*, auxin, membrane trafficking, PIN2, stress, vacuole.

Summary

- How plants balance growth and stress adaptation is a long-standing topic in plant biology. Abscisic acid (ABA) induces the expression of the stress-responsive Asparagine Rich Protein (NRP), which promotes the vacuolar degradation of PP6 phosphatase FyPP3, releasing ABI5 transcription factor to initiate transcription. Whether NRP is required for growth remains unknown.
- We generated an *nrp1 nrp2* double mutant, which had a dwarf phenotype that can be rescued by inhibiting auxin transport. Insufficient auxin in the transition zone and over-accumulation of auxin at the root tip was responsible for the short elongation zone and short-root phenotype of *nrp1 nrp2*.
- The auxin efflux carrier PIN2 over-accumulated in *nrp1 nrp2* and became de-polarized at the plasma membrane, leading to slower root basipetal auxin transport. Knock-out of *PIN2* suppressed the dwarf phenotype of *nrp1 nrp2*. Furthermore, ABA can induce NRP-dependent vacuolar degradation of PIN2 to inhibit primary root elongation. FyPP3 also is required for NRP-mediated PIN2 turnover.
- In summary, in growth condition, NRP promotes PIN2 vacuolar degradation to help maintain PIN2 protein concentration and polarity, facilitating the establishment of the elongation zone and primary root elongation. When stressed, ABA employs this pathway to inhibit root elongation for stress adaptation.

Introduction

The land plants are sessile organisms. When facing abiotic and biotic stresses, they have to decide on whether to continue growth or to balance between growth and stress response (Gong *et al.*, 2020). When the stress is really severe, plants may switch from growth to stress adaptation for survival. Identifying the molecular switches, and elucidating their individual underlying signaling pathways, not only is critical in understanding the survival strategies of plants, but also may serve as the basis for breeding crops that exhibit stress resistance with reduced yield penalty (Bailey-Serres *et al.*, 2019).

We have previously characterized two such signaling pathways, both featuring the land plant-specific, stress-responsive Asparagine Rich Protein (NRP). In the first pathway, the fungal pathogen *Verticillium dahliae* infects *Arabidopsis* and secretes an effector protein PevD1. PevD1 has a 3D structure resembling the C2 domain of membrane trafficking regulators. After entering the cell via endocytosis, PevD1 competes with the blue-light receptor Cryptochrome 2 (CRY2) for the binding of NRP.

Consequently, CRY2, freed from the cytoplasmic retention by NRP, shuttles back into the nucleus to trigger early flowering (Zhou *et al.*, 2017). In the second pathway, the abiotic stress hormone ABA strongly induces the expression of NRP, which recruits phytochrome-associated serine/threonine protein phosphatase 3 (FyPP3), a catalytic subunit of the Ser/Thr PROTEIN PHOSPHATASE6 (PP6), to the SYP41/61-positive early endosome. FyPP3 then de-phosphorylates NRP, resulting in their mutual degradation in the lytic vacuole. Consequently, the degradation of FyPP3 frees the basic leucine zipper transcription factor ABSCISIC ACID INSENSITIVE 5 (ABI5) from de-phosphorylation and de-stabilization, thus initiating ABI5-dependent transcription to inhibit seed germination (Zhu *et al.*, 2018). In both pathways, NRP transduces an adverse environmental signal, modulates the subcellular localization and/or turnover of a key growth regulatory protein, and inhibits growth.

Despite an early discovery and many subsequent reports on the involvement of NRP in various stress signaling pathways (Tenhaken *et al.*, 2005; Alves *et al.*, 2011; Reis *et al.*, 2011, 2016; Yang *et al.*, 2021), how NRP manages to participate in multiple

pathways is still enigmatic (de Camargos *et al.*, 2018). Both the N-terminal and the C-terminal amino acid sequence of the protein are unique: the N-terminus is highly disordered and rich in asparagine (~25% in amino acid sequence, hence the name NRP), and the C-terminus is composed of a Development and Cell Death (DCD) domain, which is conserved in the land plants, yet without a well-defined molecular function (Tenhaken *et al.*, 2005).

Meanwhile, how the versatile PP6 is recruited by different interacting partners to trigger different signaling routes also awaits exploration. In eukaryotes, serine/threonine phosphorylation is catalyzed by hundreds of kinases, whereas > 90% of dephosphorylation is achieved by a small family of phosphoprotein phosphatases (PPP) (Uhrig *et al.*, 2013). The PPP family is mainly composed of PP1, PP2A, PP2B, PP4, PP5, PP6 and PP7 in mammals and plants, and the PPP catalytic subunits are in general recruited by noncatalytic subunits/adaptor proteins to form multimeric holoenzymes (Uhrig *et al.*, 2013; Lillo *et al.*, 2014). The noncatalytic subunits and adaptors are large in number and vary in sequences and structures. Arabidopsis has two PP6 catalytic subunits, PP6-1/FyPP1 and PP6-3/FyPP3, with nearly identical amino acid sequences (Dai *et al.*, 2012, 2013a). They were first identified as phosphatases that interact and dephosphorylate the phytochromes, thus regulating flowering time (Kim *et al.*, 2002). A recent study further illuminated the function of PP6 in repressing photomorphogenesis by controlling the phosphorylation, stability and transcription of PHYTOCHROME-INTERACTING FACTORS (PIFs) (Yu *et al.*, 2019). Apart from its regulatory roles in light-mediated growth, PP6 also is a key player in auxin-mediated polarized growth and ABA-mediated stress adaptation (Li *et al.*, 2011; Dai *et al.*, 2012, 2013b). FyPP1/3 antagonizes PINOID (PID) and de-phosphorylates the auxin efflux carrier proteins, PIN FORMED 1 and 2 (PIN1 and PIN2), to facilitate the basal localization of PIN at the plasma membrane, thus promoting acropetal auxin transport at the root tip. Disruption of FyPP1/3 activity leads to basal-to-apical shift of PIN and auxin deficiency at the root tip (Dai *et al.*, 2012). In the developing leaf, FyPP1 also antagonizes PID by de-phosphorylating PIN1, and the kinase–phosphatase switch controls PIN1 targeting at the tip of the pavement cell lobes, leading to proper establishment of pavement cell morphogenesis (Li *et al.*, 2011). In ABA signaling, FyPP1/3 interacts and de-phosphorylates ABI5 to promote its degradation. Disruption of FyPP1/3 activity thus results in ABA hypersensitivity and growth inhibition (Dai *et al.*, 2013b). The fact that PP6 plays a positive role in polar auxin transport and a negative role in ABA signaling lead us to two questions: Can these two roles be intrinsically connected by a second protein? And Can NRP be the key interacting partner that determines the presence/absence of PP6 function, thus switching from auxin-mediated growth to ABA-mediated growth inhibition upon stress?

PIN proteins are rate-limiting factors in polar auxin transport (Petrasek *et al.*, 2006). Their phosphorylation status and apical-basal polar distribution are interconnected and regulated by multiple protein kinases and phosphatases, including AGC kinases

(D6PK and PID) and MAP kinases (MPK3/6) (Friml *et al.*, 2004; Barbosa *et al.*, 2014; Jia *et al.*, 2016; Weller *et al.*, 2017), and PP1, PP2A and PP6 phosphatases (Michniewicz *et al.*, 2007; Dai *et al.*, 2012; Guo *et al.*, 2015; Karampelias *et al.*, 2016; Li *et al.*, 2020). The subcellular distribution of PIN proteins is determined by constitutive vesicle trafficking between the plasma membrane (PM) and the endosome (Geldner *et al.*, 2001; Dhonukshe *et al.*, 2007) as well as vacuolar degradation (Kleine-Vehn *et al.*, 2008). In addition, PIN proteins can translocate between different sides of the cell (transcytosis) to rapidly induce differential growth, such as in gravitropism and phototropism (Kleine-Vehn *et al.*, 2010). Salt stress and osmotic stress can induce clathrin-mediated endocytosis of PIN2, leading to asymmetrical auxin distribution and halotropism (Galvan-Ampudia *et al.*, 2013; Zwiewka *et al.*, 2015). Our previous observation on the ABA-induced, NRP-dependent endocytosis of FyPP3 suggested that NRP could play a role in endo-lysosomal trafficking (Zhu *et al.*, 2018), and thus we speculate that the distribution of PIN proteins could be regulated by both NRP and FyPP3.

Here we further elaborate the function of both NRP and FyPP3 in the ABA–auxin interplay. First, an unexpected, house-keeping role of NRP in auxin-mediated growth was identified. The *nrp1 nrp2* double mutant over-accumulated auxin at its root tip and had a short-root phenotype, which was significantly restored by auxin transport inhibitor N-1-naphthylphthalamic acid (NPA). A much shorter elongation zone (EZ) was observed in the double mutant, and the auxin response marker *DR5:3×VENUS* was barely detectable in the epidermal cells of EZ, indicating a reduction of auxin flux into the EZ. Consistently, excess PIN2-GFP signals were observed at the lateral plasma membrane (PM) and inside the cells, resulting in PIN2 depolarization. Using the vesicle trafficking inhibitor Brefeldin A (BFA) and vacuolar H⁺-ATPase inhibitor Cocanamycin A (ConA), we found out that NRP may function in PIN2 transcytosis and vacuolar degradation, thus promoting polar auxin transport. Furthermore, ABA promotes PIN2 vacuolar degradation rather than recycling back to the PM in an NRP-dependent way, likely repressing auxin transport and primary root elongation under stress conditions. We also found out that the function of NRP in auxin distribution is likely dependent on FyPP3, as suppressing NRP and FyPP3 functions simultaneously resulted in a wild-type-like phenotype. RNA sequencing further consolidated the positive and negative regulatory roles for NRP and FyPP3 in ABA-mediated signaling. Interestingly, loss of both NRP and FyPP3 function led to downregulation of the genes encoding plasma membrane-localized proteins, especially the auxin flux carriers, and ABA treatment overruled such downregulation. Meanwhile, the SAUR19-24 subfamily of auxin-induced SMALL AUXIN UP-RNA (SAUR) genes, key players in cell elongation and tropism (Spartz *et al.*, 2014; Wang *et al.*, 2020), were repressed in both *nrp* and *FyPP3-DN*, yet strongly induced in ABA-treated *nrp/FyPP3-DN*, indicating that the suppression of auxin-mediated growth by ABA is at least partly mediated by the NRP-FyPP3 module. In summary, NRP is required for both growth and stress response, and ABA employs NRP not only in a signaling pathway, but also in a trafficking pathway, to achieve stress adaptation.

Materials and Methods

Accession numbers

NRP1 (AT5G42050), NRP2 (AT3G27090), FyPP3 (AT3G19980), PIN1 (AT1G73590), PIN2 (AT5G57090), TIP4;1-like (AT4G34270), SYP43 (AT3G05710), SYP61 (AT1G28490), VAMP727 (AT3G54300), TIP3;1 (AT1G73190), EF1a (AT5G60390).

Plant materials and growth conditions

Arabidopsis thaliana Ecotype Columbia-0 (Col-0) were used for all experiments. Double mutants *nrp1 nrp2* were generated by crossing using *nrp1* (SALK_041306) and *nrp2* (GK_520C04) (NRP, Asparagine Rich Protein). *nrp1 nrp2* homozygotes were isolated from the F₃ population by PCR and confirmed by reverse transcription (RT)-PCR. *Pro35S:FyPP3DN-RFP*, *DR5rev:GFP*, *DR5:3×VENUS*, *ProIAA2:GUS*, *PIN1-GFP* and *PIN2-GFP* were reported previously (Swarup *et al.*, 2001; Benkova *et al.*, 2003; Heisler *et al.*, 2005; Xu & Scheres, 2005; Dai *et al.*, 2013b; Zhu *et al.*, 2018) (RFP, red fluorescent protein; GFP, green fluorescent protein; GUS, β -glucuronidase). These lines were crossed with *nrp1 nrp2* and the progenies were identified by genomic PCR and confirmed by RT-PCR. Primers used in this study were listed in Supporting Information Table S1.

Generally, *Arabidopsis* seeds were surface-sterilized with 75% ethanol for 5 min, rinsed with distilled water for five times, then stratified at 4°C for 2 d before plating on ½ Murashige & Skoog medium containing 0.8% (w/v) agar, 1% (w/v) sucrose, pH 5.7. The plants then were grown in a 16 h : 8 h, light : dark, 22°C : 18°C photoperiod with a photosynthetic photon flux density of 100 $\mu\text{mol m}^{-2} \text{s}^{-1}$. Soil-grown plants were kept under the same conditions.

Constructs and transgenic lines

In order to complement *nrp1 nrp2*, *Pro35S:NRP1-GFP* was introduced into the double mutant by floral dipping as described previously (Zhu *et al.*, 2018). The transgenic lines were screened using 25 mg l⁻¹ hygromycin and verified with PCR and RT-PCR.

For the *nrp1 nrp2 pin1* and *nrp1 nrp2 pin2* lines, *pin1* and *pin2* were crossed with *nrp1 nrp2*, respectively (PIN, PIN FORMED). Triple mutants were identified by genomic PCR and confirmed by RT-PCR.

For the *NRP1-mCherry* line, the *NRP1-mCherry* fusion gene was cloned to *pCambia1302* vector under the control of the 35S promoter and was introduced into the *A. thaliana* by floral dipping. The transgenic lines were screened using 25 mg l⁻¹ hygromycin and verified with PCR and fluorescence.

For the *PIN2-GFP VAMP727-mRuby* and *nrp1 nrp2 NRP1-GFP VAMP727-mRuby* lines, *PIN2-GFP* and *nrp1 nrp2 NRP1-GFP* were crossed with *VAMP727-mRuby* and the progenies were identified by PCR and fluorescence.

In order to observe endocytosis and exocytosis of *FyPP3DN PIN2-GFP*, *nrp1 nrp2 FyPP3DN PIN2-GFP* and *nrp1 nrp2 FyPP3DN PIN1-GFP*, all of the transgenic lines were generated by crossing *Pro35S:FyPP3DN-RFP* (Zhu *et al.*, 2018) into *PIN2-GFP*, *nrp1 nrp2 PIN2-GFP* and *nrp1 nrp2 PIN1-GFP* transgenic plants (FyPP3, phytochrome-associated serine/threonine protein phosphatase 3). The transgenic lines were screened using 25 mg l⁻¹ hygromycin and verified with PCR and RT-PCR.

In order to observe FM4-64 staining of *FyPP3DN DR5:3×VENUS* and *nrp1 nrp2 FyPP3DN DR5:3×VENUS*, and *FyPP3DN PIN2-GFP* and *nrp1 nrp2 FyPP3DN PIN2-GFP* in darkness, *pUBQ10:FyPP3DN-BFP* was constructed using *Pro35S:FyPP3DN-RFP* as the template. The construct was introduced into *DR5:3×VENUS*, *nrp1 nrp2 DR5:3×VENUS*, *PIN2-GFP* and *nrp1 nrp2 PIN2-GFP* by floral dipping. Primary transformants were selected by 25 mg l⁻¹ hygromycin and verified with PCR and RT-PCR.

For the *nrp1 nrp2 FyPP3-OE PIN2-GFP* line, *pUBQ10:FyPP3-BFP* was constructed using *Pro35S:FyPP3-RFP* (Zhu *et al.*, 2018) as the template and *pCambia1302* as the vector. The construct was introduced into *Agrobacterium tumefaciens* (GV3101) for floral dipping. Primary transformants were selected by 25 mg l⁻¹ hygromycin and verified with PCR and RT-PCR.

In order to conduct fluorescence co-localization and co-immunoprecipitation (CO-IP) experiments using transgenic lines *nrp1 nrp2 NRP1-mCherry FyPP3DN PIN2-GFP*, *nrp1 nrp2 NRP1-mCherry FyPP3-OE PIN2-GFP* and *nrp1 nrp2 NRP1-mCherry PIN2-GFP*, the *NRP1-mCherry* line was crossed with *nrp1 nrp2 FyPP3DN PIN2-GFP*, *nrp1 nrp2 FyPP3-OE PIN2-GFP* and *nrp1 nrp2 PIN2-GFP*, respectively. The progenies were identified by genomic PCR and confirmed by RT-PCR. Primers used in this study are all listed in Table S1.

Phenotypes of seedlings were captured with a scanner (Perfection V33; Epson, Nagano, Japan). Soil-grown plants were photographed with a digital camera (Powershot A800; Canon, Tokyo, Japan).

Detailed descriptions of materials and methods are included in Methods S1.

Results

Knocking-out of NRP1/2 leads to over-accumulation of auxin at the root tip

The *Arabidopsis* NRP (At5g42050) has a close homologue, At3g27090, that is 80% identical in the DCD domain (Tenhaken *et al.*, 2005; Zhou *et al.*, 2017). We followed Reis *et al.* and renamed NRP NRP1 and At3g27090 NRP2 (Reis *et al.*, 2016). In addition to *nrp1* (Salk_041306) (Zhou *et al.*, 2017; Zhu *et al.*, 2018), a T-DNA insertion line for *NRP2*, GK_520C04, was obtained, and an *nrp1 nrp2* double mutant was generated by crossing, and verified by RT-PCR (Fig. S1A, B). Like *nrp1*, *nrp2* has a slightly longer primary root than the wild-type (WT) (Fig. 1a,b). Surprisingly, the *nrp1 nrp2* double mutant had a dwarf phenotype, with smaller cotyledons and

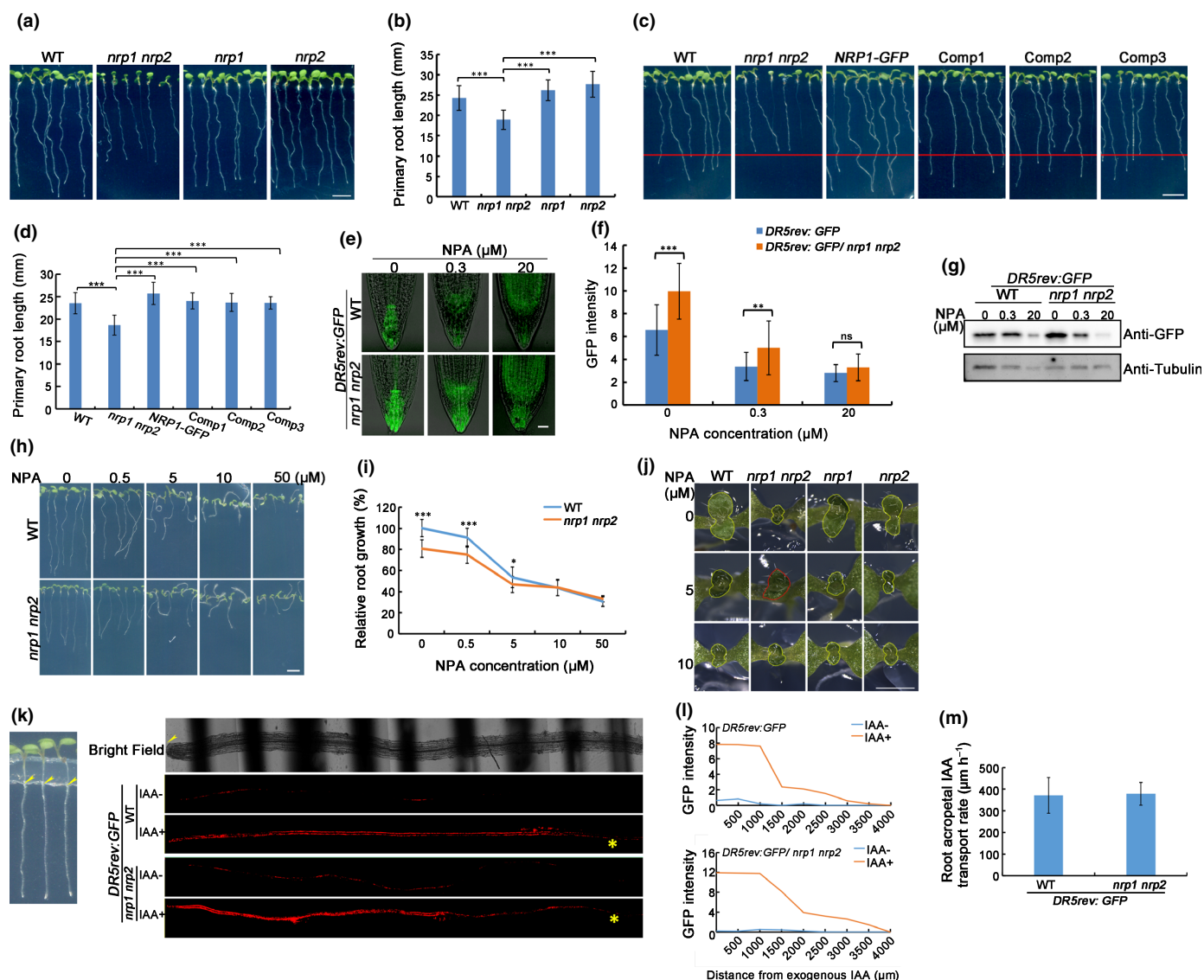


Fig. 1 The *nrp1 nrp2* double mutant has short primary root and accumulates auxin at the root tip (NRP, Asparagine Rich Protein). (a) Seven-d-old, vertically grown Arabidopsis wild-type (WT), *nrp1 nrp2*, *nrp1* and *nrp2* seedlings. (b) Quantification of primary root length of seedlings in (a). (c) Complementation of *nrp1 nrp2* with *Pro35S:NRP1-GFP* (GFP, green fluorescent protein). Three representative complementation lines, Comp1, Comp2 and Comp3, are shown. *Pro35S:NRP1-GFP* also was used for comparison. (d) Quantification of primary root length of seedlings in (c). (e) Laser scanning confocal microscopy (LSCM) images of *DR5rev:GFP* in WT and *nrp1 nrp2* backgrounds, grown vertically with 0, 0.3 and 20 μM N-1-naphthylphthalamic acid (NPA) for 5 d. Identical scanning parameters were used. (f) Quantification of integrated GFP fluorescence intensity in (e). (g) Immunoblotting of GFP with root tips (0.5 mm each) collected from (e). Beta-tubulin was used as loading control. (h) Seven-d-old WT and *nrp1 nrp2* seedlings, grown vertically on plates containing various concentrations of the polar auxin transport inhibitor NPA. (i) Quantification of reduction in primary root elongation of WT and *nrp1 nrp2* in (h). The root length of WT without NPA was set to 100%. (j) Top view of the 7-d-old seedlings showing the first pair of true leaves (yellow dotted lines). Note the restored leaf size in *nrp1 nrp2* grown on 5 μM NPA (red dotted lines). (k) In 5-d-old vertically grown seedlings, root acropetal auxin transport rate was inferred by documenting the *DR5rev:GFP* fluorescence intensity along the primary root towards the root tip (yellow stars), 13 h after agar strips containing 0 (IAA-) or 100 μM IAA (IAA+) were placed below the shoot-root junction (yellow arrowheads). (l) Quantification of the *DR5rev:GFP* fluorescence intensity along the primary root towards the root tip of WT and *nrp1 nrp2* in (k). (m) Calculated root acropetal auxin transport rate in WT and *nrp1 nrp2*. Bars: (a, c, h) 5 mm; (e) 25 μm; (j) 0.5 mm. Vertical lines in (b), (d), (f), (i) and (m) indicate SD. ***, $P < 0.001$; **, $P < 0.01$; *, $P < 0.05$; ns, nonsignificant (Student's *t*-test). Quantification was done with ≥ 30 roots from three biological replicates in (b), (d), (f) and (i), and with eight roots in (k).

true leaves, and a significantly shorter primary root compared with the WT (Fig. 1a,b). In the soil, *nrp1 nrp2* was much slower in growth and senesced early (Fig. S2A,B). Similar early senescence phenotypes had been observed in *FyPP1/3* over-expression lines (Dai *et al.*, 2013a), suggesting that *NRP1/2*

may antagonize *FyPP1/3* not only in stress response but in growth regulation. The phenotypes of the double mutant were completely restored by complementation with *Pro35S:NRP1-GFP* (*NRP1-OE*) (Figs 1c,d, S2B,C). These observations indicated that, apart from a positive role in stress response, *NRP1*

and 2 also may act redundantly as positive, rather than negative, growth regulators.

In fact, *FyPP1/3* is required not only for inhibition of ABA signaling, but also for PIN de-phosphorylation and acropetal auxin transport in the primary root (Dai *et al.*, 2012). To test this, we introduced the auxin response reporter *DR5rev:GFP*, *DR5:3×VENUS* and *ProIAA2:GUS* into *nrp1 nrp2* (Swarup *et al.*, 2001; Benkova *et al.*, 2003), separately, and then analyzed the auxin responses in the double mutant with or without auxin or auxin efflux inhibitor N-1-naphthylphthalamic acid (NPA) (Geldner *et al.*, 2001). Indeed, the intensity of *DR5rev:GFP* was significantly higher in the quiescent center (QC) and the columella cells of *nrp1 nrp2* than in the WT (Fig. 1e–g), indicative of an over-accumulation of auxin at the root tip. Such a difference was reduced by NPA treatment: 0.3 μ M NPA could reduce the fluorescence intensity of GFP (and the GFP concentration) in *nrp1 nrp2/DR5rev:GFP* to a level comparable to that observed in the WT on $\frac{1}{2}$ MS (Fig. 1e–g); and the difference in the primary root length was gradually reduced as the NPA concentration went up (Fig. 1h,i). Notably, 5 μ M NPA promoted the expansion of true leaves in *nrp1 nrp2*, indicative of a replenishment of endogenous auxin in the shoot (Fig. 1j).

In order to rule out the possibility that the higher *DR5rev:GFP* signal at the root tip of the double mutant is due to excessive auxin biosynthesis, the seedlings were treated with two auxin biosynthesis inhibitors, L-Kynurenine (L-Kyn) and 4-phenoxyphenylboronic acid (PPBo). L-Kyn and PPBo were identified through screening for inhibitors for Tryptophan aminotransferase of Arabidopsis 1/Tryptophan aminotransferase relateds (TAA1/TARs) and YUCCA, the two enzymes in the indole-3-pyruvate (IPyA) pathway of auxin biosynthesis (He *et al.*, 2011; Kakei *et al.*, 2015). No difference between *nrp1 nrp2* and the WT in the inhibition of primary root elongation was observed on either inhibitor (Fig. S3A,B,E,F). As the concentration of inhibitors used went up from 0 to 5 μ M, the DR5 signal dampened in both *nrp1 nrp2* and the WT, as expected, yet *nrp1 nrp2* always had a significantly higher DR5 signal than the WT (Fig. S3C,D,G,H), precluding the possibility that the high DR5 signal intensity in the double mutant was due to excessive auxin biosynthesis at the root tip.

The possibility that the higher DR5 signal is due to a higher auxin response in *nrp1 nrp2* also was ruled out. The *nrp1 nrp2/ProIAA2:GUS* seedlings treated with IAA produced identical staining patterns with *ProIAA2:GUS* in the WT background (Fig. S4A). Also, increments in GFP or VENUS fluorescence intensities of both *DR5rev:GFP* and *DR5:3×VENUS* was comparable in the *nrp1 nrp2* and WT backgrounds following exogenous NAA and 2,4-D treatment (Fig. S4B,C). Lastly, consistent with the imaging results, no significant difference on primary root elongation was observed between the double mutant and the WT grown on series of concentrations of IAA, NAA or 2,4-D (Fig. S4D–F).

Finally, the rate of root basipetal and acropetal IAA transport was measured in *nrp1 nrp2* and WT carrying *DR5rev:GFP*. The seedlings were transferred to vertical plates, and an agar block containing IAA was placed onto the root tips or the root-hypocotyl

junction (Figs 1k, S5A). Thirteen hours later, the seedlings were scanned with laser scanning confocal microscopy (LSCM), and the GFP signal intensity along the root, either upward or downward, was quantified. Root acropetal IAA transport rate was comparable in *nrp1 nrp2* and WT (Fig. 1k–m). After applying IAA onto root tips for basipetal IAA transportation, signal intensity of *DR5rev:GFP* in the transition zone appeared higher in *nrp1 nrp2*. DR5 signal in the elongation zone, however, was much lower in *nrp1 nrp2* compared to the WT (Fig. S5A,B).

We therefore concluded that *nrp1 nrp2* had too much auxin at the root tip due to abnormal auxin transport rather than auxin biosynthesis or response. Specifically, the basipetal auxin transport into the elongation zone was clearly slowed down.

Loss of NRP leads to cytosolic accumulation of PIN2

The auxin efflux carriers PIN1 and PIN2 are vital in primary root elongation and the establishment of the elongation zone, and both are dynamic membrane proteins that consistently get produced, secreted, modified, recycled and degraded. To see if they are the major players behind the short-root phenotype of *nrp1 nrp2*, we crossed *nrp1 nrp2* with *pin1* and *pin2*, separately, to generate triple mutants. *nrp1 nrp2 pin1* inherited the dwarf phenotype of *nrp1 nrp2* and the pin-like inflorescence phenotype of *pin1*, exhibiting a synthetic phenotype (Fig. S6). *nrp1 nrp2 pin2*, however, looked like the WT (Fig. 2a–c), suggesting that NRPs and PIN2 function antagonistically in the same pathway to regulate growth.

nrp1 nrp2 PIN2-GFP then was generated to examine the possible changes in PIN2-GFP amounts and distribution in *nrp1 nrp2*. PIN2-GFP intensity was significantly elevated in the double mutant, and apart from the apical plasma membrane (PM), strong PIN2 signal was observed at the lateral PM (Fig. 2d,e). Additionally, cytoplasmic PIN2-GFP puncta accumulated in *nrp1 nrp2* (Fig. 2d,e). Immunoblotting also confirmed the over-accumulation of PIN2-GFP in *nrp1 nrp2* root tips (Fig. 2f).

PIN1-GFP intensity was much lower in *nrp1 nrp2*, yet the polar PM distribution of PIN1 in *nrp1 nrp2* was not significantly different from that of the WT (Fig. S7A,B).

We then treated the seedlings with the vesicle trafficking inhibitor Brefeldin A (BFA) (Geldner *et al.*, 2001), and also performed BFA washout, to observe the rate of endocytosis and exocytosis of PIN2. Consistent with the observation that *nrp1 nrp2* had more cytoplasmic PIN2-GFP puncta (Fig. 2d,e), PIN2 accumulated more quickly and formed larger BFA compartments in *nrp1 nrp2* than in WT (Fig. 2g–i). The BFA compartments also were more resistant to washout in the double mutant, indicating the existence of an endosomal pool of PIN2 that is not destined to undergo exocytosis (Fig. 2g–i). Persistence of PIN1 in BFA compartments also was observed during washout (Fig. S7C,D).

We previously had shown that NRP can localize to trans-Golgi network (TGN) before its vacuolar turnover (Zhu *et al.*, 2018). To see if NRP can co-localize with and directly interact with PIN2, we generated *PIN2-GFP NRP1-mCherry*, *PIN2-GFP VAMP727-mRuby* and *NRP1-GFP VAMP727-mRuby* lines and examined co-localization of PIN2, NRP1 and VAMP727, an

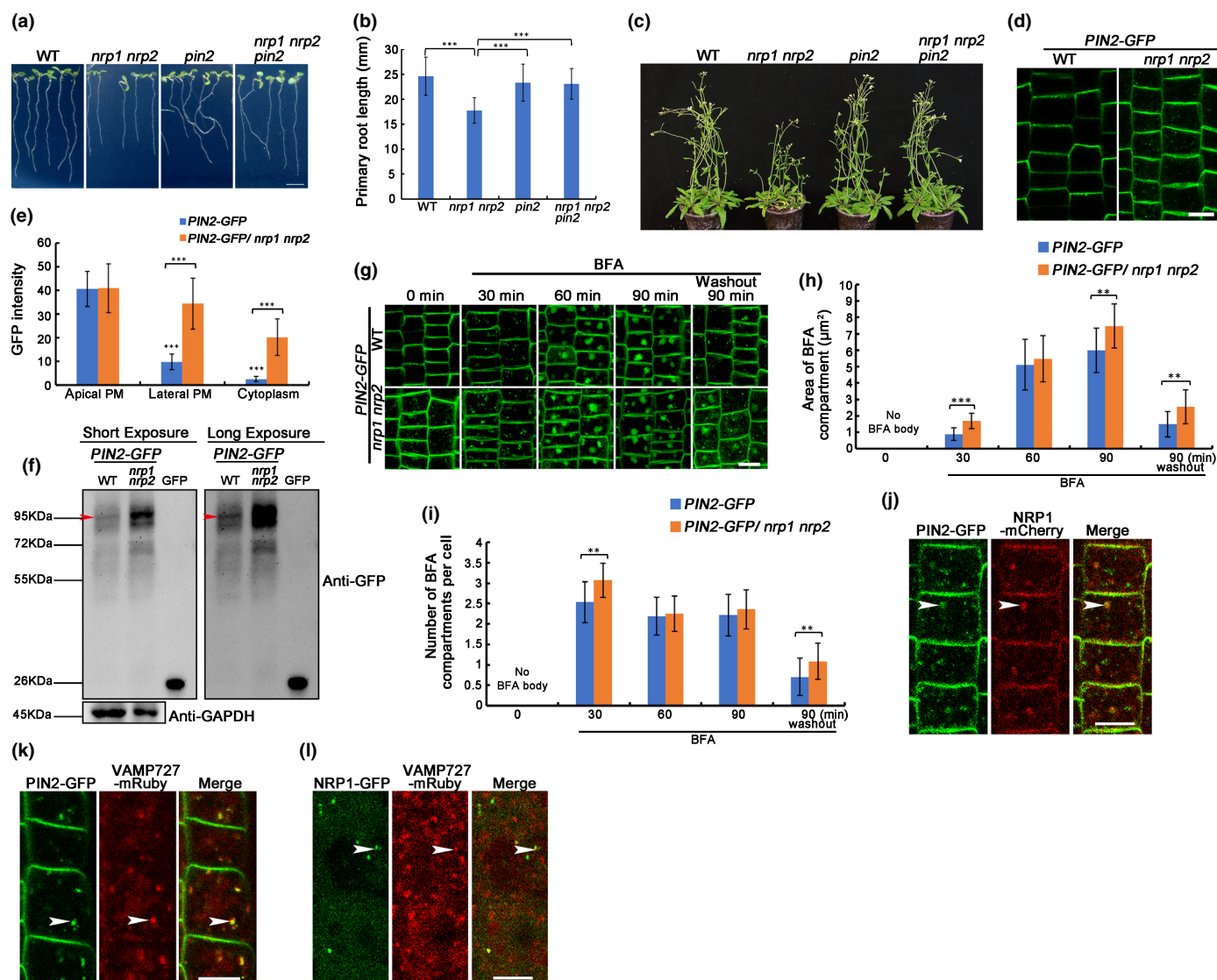


Fig. 2 Loss of Asparagine Rich Protein (NRP) function leads to over-accumulation and polarity defects of PIN-FORMED (PIN)2. (a) Seven-day-old, vertically grown Arabidopsis seedlings of wild-type (WT), *nrp1 nrp2*, *pin2* and *nrp1 nrp2 pin2*. (b) Quantification of the primary root length of the seedlings in (a). (c) Five-week-old plants; three plants in each pot. (d) Laser scanning confocal microscopy (LSCM) images of PIN2-GFP in the transition zone of root epidermis of 5-d-old WT and *nrp1 nrp2* with identical scanning parameters (GFP, green fluorescent protein). (e) Quantification of integrated fluorescence intensity of apical plasma membrane (PM), lateral PM and cytoplasmic PIN2-GFP in (d). (f) Immunoblotting of PIN2-GFP with root tips (3 mm each) collected from 5-d-old seedlings. *DR5rev:GFP* was used as GFP control. GAPDH was used as loading control. Short and long exposure times were used to illustrate the difference in PIN2-GFP protein concentrations. (g) Brefeldin A (BFA) treatment (50 μM) on WT and *nrp1 nrp2* carrying PIN2-GFP, pretreated with CHX (50 μM , 90 min), and subsequent BFA washout. (h) Quantification of the size of the BFA compartments in (g). (i) Quantification of the number of the BFA compartments in (g). (j) Partial co-localization of PIN2 and NRP1 at cytosolic puncta in the root epidermal cells of 5-d-old *nrp1 nrp2* NRP1-mCherry PIN2-GFP seedlings pretreated with abscisic acid (ABA) (100 μM , 60 min). Arrowheads indicate co-localization. (k) Partial co-localization of PIN2 and the trans-Golgi network (TGN)-localized R-SNARE VAMP727 in VAMP727-mRuby/PIN2-GFP seedlings, pretreated with ABA. Arrowheads indicate co-localization. (l) Partial co-localization of NRP1 and VAMP727 at cytosolic puncta in the root epidermal cells from *nrp1 nrp2* NRP1-GFP VAMP727-mRuby, pretreated with ABA. Arrowheads indicate co-localization. Bars: (a) 5 mm; (d, g, j, k, l) 10 μm . Diameter of pot 6.5 cm in (c). Vertical lines in (b), (e), (h) and (i) indicate SD. ***, $P < 0.001$; **, $P < 0.01$ (Student's *t*-test). At least 20 roots were measured from three biological replicates in (b). At least 30 cells from five different roots were measured in each of the three biological replicates in (e), (h) and (i).

R-SNARE that marks a vacuolar trafficking subregion of TGN and pre-vacuolar compartment (PVC) (Ebina *et al.*, 2008; Shimizu *et al.*, 2021). Partial co-localization was observed for PIN2, NRP1 and VAMP727 (Fig. 2j–l); however, direct interaction between PIN2 and NRP1 was not detected (Fig. S8). Together, our observation suggested that NRP negatively regulates PIN2 protein concentrations, likely by promoting its vacuolar degradation.

NRP is required not only for auxin-mediated growth but for ABA-induced growth inhibition

Previous studies have placed PIN2 and the elongation zone at the center stage in the interplay between ABA and auxin (Belin *et al.*, 2009; Rowe *et al.*, 2016). The *pin2* mutant is insensitive to ABA in embryonic axis elongation during germination, and ABA

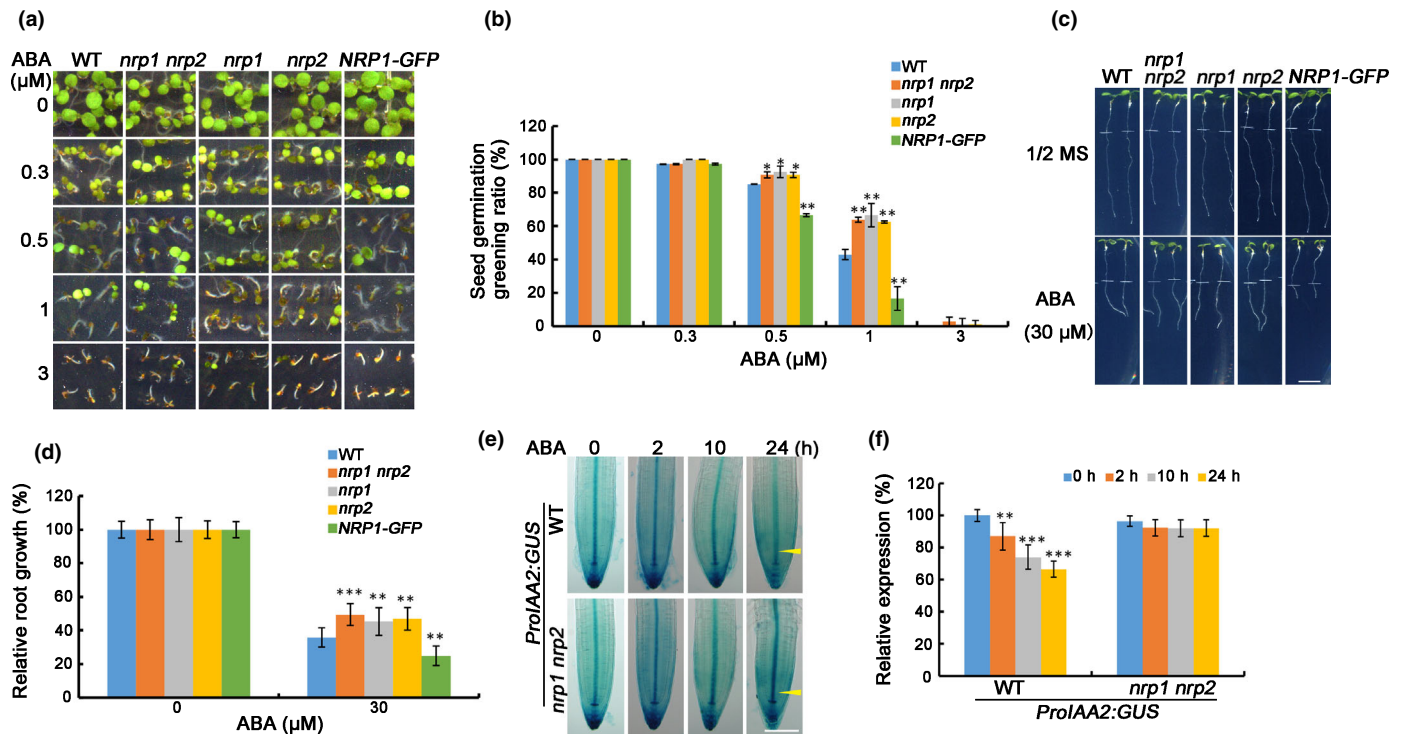


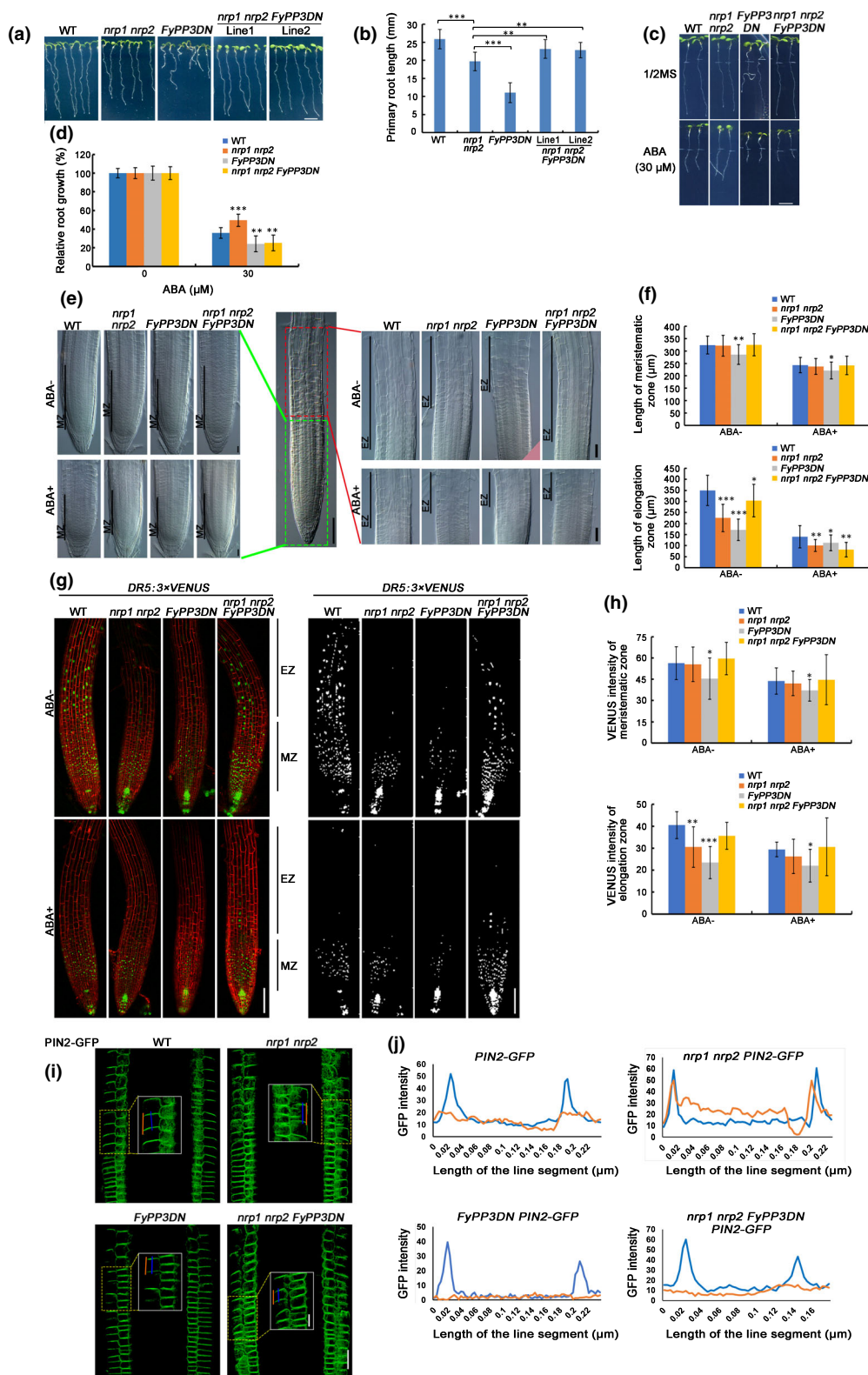
Fig. 3 The *nrp1 nrp2* double mutant is insensitive to abscisic acid (ABA) (NRP, Asparagine Rich Protein). (a) Seven-d-old Arabidopsis seedlings of WT, *nrp1 nrp2*, *nrp1*, *nrp2* and *NRP1-GFP* germinated on different concentrations of ABA. (b) Quantification of germination percentage (cotyledon greening) in (a). (c) Inhibition of primary root elongation by ABA. Four-d-old, vertically grown WT, *nrp1 nrp2*, *nrp1*, *nrp2*, and *NRP1-GFP* seedlings were transferred to 1/2 Murashige & Skoog plates (upper panel) or 1/2MS containing 30 μ M ABA (lower panel), and additional primary root elongation was scored 4 d later (GFP, green fluorescent protein). (d) Additional primary root elongation on ABA vs that on 1/2MS was calculated as relative root growth to show the inhibitory effects of ABA on primary root growth. (e) Histochemical staining of *ProIAA2:GUS* in 5-d-old WT and *nrp1 nrp2* treated with 5 μ M ABA in a 24 h time course. Yellow arrowheads indicate the difference in β -glucuronidase (GUS) intensity at the root tip region (columella, quiescent center and stele). (f) Changes of GUS intensity in response to ABA treatment over 24 h in seedlings shown in (e) were quantified. Bars: (c) 5 mm; (e) 100 μ m. Vertical lines in (b), (d) and (f) indicate SD. ***, $P < 0.001$; **, $P < 0.01$; *, $P < 0.05$ (Student's *t*-test). Germination percentage was scored from ≥ 100 seeds from three biological replicates in (a). Quantification was done with ≥ 15 roots from three biological replicates in (d). GUS intensity was quantified from ≥ 10 roots from one of three biological replicates in (e).

activates IAA2 to potentiate auxin responses in the elongation zone (Belin *et al.*, 2009). By inducing PIN2 accumulation and repressing PIN1 accumulation, osmotic stress and ABA reduce auxin concentrations in the elongation zone (Rowe *et al.*, 2016). The significant changes in PIN2 abundance and distribution in *nrp1 nrp2* prompted us to examine the possible involvement of NRP in ABA-induced inhibition of root growth, and to see whether such a role is achieved through the manipulation of PIN2. Like the *nrp1* single mutant which exhibits a typical ABA-insensitive phenotype (Zhu *et al.*, 2018), *nrp1 nrp2* was slightly insensitive to ABA in the germination assay (Fig. 3a,b). Primary root elongation in response to ABA treatment gave similar yet stronger results, with *nrp1 nrp2*, along with the single mutants, appeared insensitive (Fig. 3c,d). Although ABA gradually reduced GUS staining in the root tip region of *ProIAA2:GUS*, such reduction was not observed in the *nrp1 nrp2* background (Fig. 3e,f).

In order to better describe the role of NRP in the ABA–auxin interplay on primary root elongation, and to see if *FyPP3* also is involved, *nrp1 nrp2 FyPP3DN* lines were generated, and *DR5:3×VENUS* and *PIN2-GFP* also were introduced into these lines. *FyPP3DN* (*FyPP3 D81N*) was the same dominant negative line used in previous studies (Dai *et al.*, 2012; Zhu *et al.*, 2018).

The short-root and the agravitropism phenotype observed in *nrp1 nrp2* and *FyPP3DN* were both fully restored in *nrp1 nrp2 FyPP3DN* (Fig. 4a,b). Similar to the germination phenotype previously observed in *nrp* and *FyPP3DN* (Zhu *et al.*, 2018), primary root elongation of *nrp1 nrp2* was ABA-insensitive and *FyPP3DN* was ABA-sensitive (Fig. 4c,d). *nrp1 nrp2 FyPP3DN* also was sensitive to ABA (Fig. 4c,d).

Quantification of the lengths of the meristematic zone (MZ) and the elongation zone (EZ) confirmed that, the EZ, but not the MZ, was significantly shorter in *nrp1 nrp2* compared with the wild-type (Fig. 4e,f). In agreement with the short EZ phenotype, *DR5:3×VENUS* signals were barely detectable in the EZ of *nrp1 nrp2*, whereas strong *DR5:3×VENUS* signals were observed at the MZ, columella, and the stele of *nrp1 nrp2* (Fig. 4g; Video S1). ABA strongly reduced the length of the EZ in WT, however, to a lesser extent in *nrp1 nrp2* (Fig. 4e, f). *FyPP3DN* had a short EZ that is ABA-sensitive, and the EZ of *nrp1 nrp2 FyPP3DN* was comparable to WT yet sensitive to ABA (Fig. 4e,f). Consistently, ABA suppressed the *DR5:3×VENUS* signals in both the MZ and the EZ of the WT, yet the signals were less inhibited in *nrp1 nrp2* (Fig. 4g, h). The *nrp1 nrp2 FyPP3DN* was similar to WT in



DR5:3×VENUS intensity and distribution (Fig. 4g,h). The polar, apical PM distribution of PIN2 in the root epidermal cells also was restored to WT status in *nrp1 nrp2 FyPP3DN* (Fig. 4i,j).

These observations supported a positive role of NRP in ABA signaling and a positive role of NRP in promoting auxin flux into the EZ, and thus explained why *nrp1 nrp2* had a short primary root, yet was insensitive to exogenous ABA in primary root

Fig. 4 Loss of phytochrome-associated serine/threonine protein phosphatase 3 (FyPP3) function restores PIN-FORMED (PIN)2 distribution, auxin response and root elongation defects in *nrp1 nrp2* (NRP, Asparagine Rich Protein). (a) Loss of either NRP (*nrp1 nrp2*) or FyPP3 (*FyPP3DN*) function leads to short-root phenotype; however, loss of both (*nrp1 nrp2 FyPP3DN*) results in wild-type (WT)-like phenotype. (b) Quantification of primary root length of Arabidopsis seedlings in (a). (c) Primary root elongation of WT, *nrp1 nrp2*, *FyPP3DN* and *nrp1 nrp2 FyPP3DN* with or without exogenous abscisic acid (ABA). Four-d-old vertically grown seedlings were transferred to ½ Murashige & Skoog plates containing ABA (30 µM), and additional growth was documented 4 d later. (d) Quantification of relative root growth on ABA of seedlings in (c). (e) Effects of exogenous ABA on the meristematic zone (MZ) and the elongation zone (EZ) in each genotype. Six-d-old vertically grown seedlings were transferred to ½MS with or without ABA (30 µM) and imaged 6 h later with differential interference contrast (DIC) microscopy. (f) Quantification of the length of MZ and EZ of the seedlings in (e). (g) Auxin response, represented by DR5:3×VENUS, in the MZ and EZ of 5-d-old seedlings treated with or without ABA (30 µM, 6 h). FM4-64 was used to stain the plasma membrane. DR5:3×VENUS images were presented alone in grayscale on the right side. (h) Quantification of VENUS intensity in the MZ and EZ of the seedlings from (g). (i) Subcellular distribution of PIN2-GFP in plasmolyzed (4 M NaCl, 20 min) WT, *nrp1 nrp2*, *FyPP3DN* and *nrp1 nrp2 FyPP3DN* root tips (GFP, green fluorescent protein). To describe the cytoplasmic and plasma membrane (PM) distribution pattern of PIN2, orange lines were drawn along the edge/lateral PM of the epidermal cell, and blue lines were drawn close to the center of the cell. (j) Integrated GFP intensity along the orange and blue line segments in (i). PIN2-GFP signals were abundant at the lateral PM of *nrp1 nrp2* only. Bars: (a, c) 5 mm; (e, g) 100 µm; (i) 20 µm. Vertical lines in (d), (f) and (h) indicate SD. ***, $P < 0.001$; **, $P < 0.01$; *, $P < 0.05$ (Student's *t*-test). Quantification was done with ≥ 20 roots from three biological replicates in (b), ≥ 12 roots from three biological replicates in (f) and (h).

elongation. FyPP3 appeared to act as an opponent of NRP in regulating primary root elongation, with or without ABA.

ABA promotes NRP-mediated vacuolar degradation of PIN2

In order to further understand the function of NRP and FyPP3 on PIN2-mediated EZ formation, and to see the role of ABA in this process, we compared the concentrations, subcellular distribution, trafficking and degradation of PIN2 in *nrp1 nrp2*, *FyPP3DN* and *nrp1 nrp2 FyPP3DN* carrying *PIN2-GFP*, in combination with ABA treatment.

The first thing notable was the difference in PIN2-GFP intensities. The *nrp1 nrp2* double mutant over-accumulated PIN2-GFP both at the PM and in the cytoplasm (Figs 2d,e, 5a,b). *FyPP3DN* had a reduced PIN2-GFP intensity, and little cytoplasmic signal could be seen. PIN2-GFP intensities and distribution in *nrp1 nrp2 FyPP3DN* looked similar to WT (Fig. 5a).

ABA promoted endocytosis of PIN2-GFP in the WT and *nrp1 nrp2 FyPP3DN* (Fig. 5a,b), and further enhanced the formation of the BFA compartments within them (Fig. 5a,c). Strikingly, during BFA washout, the cytosolic PIN2 puncta disappeared faster in the presence of ABA in WT and *nrp1 nrp2 FyPP3DN* (Fig. 5a,c,d). The disappeared PIN2-GFP might have gone to the vacuole, rather than returning to the PM. Indeed, a subpopulation of PIN2-GFP was detected in the presence of the vacuolar H^+ -ATPase inhibitor Concanamycin A (Con A) during BFA washout (Fig. 5a,c,d). Similar patterns were observed during BFA washout of PIN1-GFP (Fig. S9A–C). PIN2-GFP in *nrp1 nrp2* accumulated to the BFA compartment quickly and had a tendency to stay in BFA compartment, getting washed out very slowly (Figs 2g–i, 5a–d). In addition, PIN2-GFP in *nrp1 nrp2* was insensitive to ABA, both in the presence of BFA (endocytosis) and during BFA washout (exocytosis) (Fig. 5a–d). PIN2-GFP in *FyPP3DN* formed smaller BFA compartments that washed out quickly, with ABA having little effect on them. ConA also had little impact on PIN2-GFP in *FyPP3DN* (Fig. 5a–d). The observations were further validated by immunoblotting of PIN2-GFP using root tips cut from seedlings undergone the same treatments in Fig. 5(a). During BFA washout, in the

presence of ABA, a clear reduction in PIN2-GFP was observed (Fig. 5e,f). The intensity of PIN2-GFP was restored when both ABA and ConA were present (Fig. 5e,f). Such pattern was not visible in either *nrp1 nrp2* or *FyPP3DN*, yet was seen again in *nrp1 nrp2 FyPP3DN* (Fig. 5e,f).

In order to better describe the impact of NRP on PIN2-GFP vacuolar degradation, the dark-induced PIN2 degradation process, with or without ABA treatment, was observed. At 2 h of dark incubation, many PIN2-GFP signals were observed at early and late endosomes labelled by the endocytic probe FM4-64 (Fig. 6a). At 4 h of dark treatment, most cytoplasmic PIN2-GFP signals were seen in the vacuole, outlined by FM4-64. Three hours of dark plus 1 h of ABA (CHX + ABA) treatment resulted in a large population of PIN2-GFP in the vacuole (Fig. 6b). PIN2-GFP in *nrp1 nrp2* gave interesting results: they accumulated normally in the endosomes and vacuoles in the dark. However, ABA treatment clearly prevented PIN2-GFP from getting into the vacuole. Dark treatment induced very little endocytosis of PIN2-GFP in *FyPP3DN* (Fig. 6a,b). Such insensitivity to darkness is expected because FyPP3 negatively regulates photomorphogenesis (Yu *et al.*, 2019). Upon ABA treatment, in *FyPP3DN*, the endocytosed PIN2-GFP mainly decorated the tonoplast (Fig. 6b), resembling the pattern observed in the Endosomal Sorting Complexes Required for Transport (ESCRT) mutants (Spitzer *et al.*, 2009), suggesting that FyPP3 is not a prerequisite for the ABA-induced PIN2 vacuolar degradation, even though it may have a previously unreported, positive role in regulating ESCRT machinery. Lastly, *nrp1 nrp2 FyPP3DN* responded to dark and dark plus ABA in a WT manner.

In ABA signaling, FyPP3, recruited by NRP, can dephosphorylate the latter to trigger their mutual vacuolar degradation (Zhu *et al.*, 2018). Here we also examined if FyPP3 can be a determinant of the potential interaction between PIN2 and NRP, and their subsequent vacuolar degradation. *FyPP3-OE* and *FyPP3DN* was introduced into *nrp1 nrp2 NRP1-mCherry PIN2-GFP*, and the co-localization and co-immunoprecipitation of PIN2-GFP and NRP1-mCherry were analyzed in these lines, in the presence of ABA in the dark (Figs 6c, S10). Indeed, the NRP-mediated vacuolar accumulation of PIN2 was positively dependent on FyPP3. In *FyPP3-OE*, most cytoplasmic PIN2-GFP

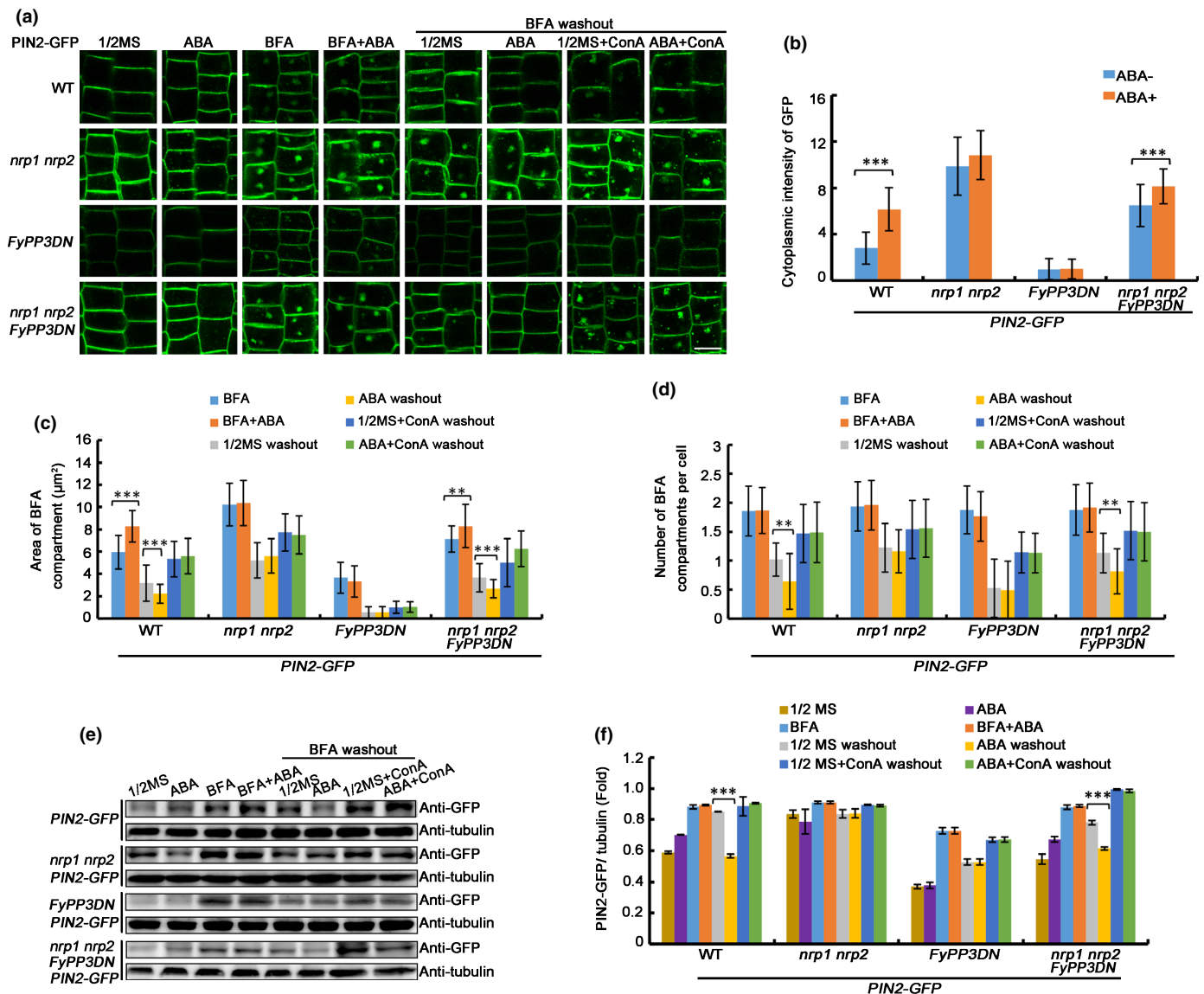


Fig. 5 Abscisic acid (ABA) promotes vacuolar degradation of PIN2-GFP in an NRP-dependent way (GFP, green fluorescent protein; NRP, Asparagine Rich Protein; PIN, PIN-FORMED). (a) Laser scanning confocal microscopy (LSCM) of PIN2-GFP in 5-d-old Arabidopsis wild-type (WT), *nrp1 nrp2*, phytochrome-associated serine/threonine protein phosphatase 3 (*FyPP3*)DN, and *nrp1 nrp2 FyPP3DN* seedlings, pretreated with 1/2 Murahsie & Skoog containing CHX (50 μM), treated with either ABA (100 μM), Brefeldin A (BFA) (25 μM), or ABA plus BFA, for 1 h. Then ABA (100 μM) and ConA (0.5 μM) were added to 1/2MS during a 30-min BFA washout. (b) Quantification of cytoplasmic PIN2-GFP signal intensity with or without ABA in (a). (c) Quantification of the size of BFA compartments in (a). (d) Quantification of the number of BFA compartments in (a). (e) PIN2-GFP accumulation in (a) was quantified by immunoblotting. Only the root tips (2 mm) were collected for immunoblotting. Anti-tubulin was used as an internal control. (f) Quantification of (e). Bars: (a) 10 μm . Vertical lines in (b), (c), (d) and (f) indicate SD. ***, $P < 0.001$; **, $P < 0.01$ (Student's *t*-test). Three biological replicates were done in (a) and (e). At least 80 cells from five roots were quantified in (a), and ≥ 100 cells from eight roots were quantified in (c) and (d).

co-localized with NRP1-mCherry in the vacuoles. In *FyPP3DN*, however, very little PIN2-GFP signal was detected in the vacuole, and NRP1-mCherry was clearly not in the vacuole. No interaction between PIN2 and NRP1 was detected in WT, *FyPP3-OE* and *FyPP3-DN* (Figs 6c, S10). The co-localization of NRP1, NRP2 and *FyPP3* with endosome markers (SYP43, SYP61, VAMP727) or the vacuole marker (TIP3;1) also was observed in the leaves of *Nicotiana benthamiana* with transient expression (Fig. S11A,B). These observations consolidated a positive role for *FyPP3* on NRP activation that leads to vacuolar degradation of PIN2 and NRP.

Transcriptome analyses support the roles of NRP and *FyPP3* in regulating both auxin-mediated growth and ABA-induced growth suppression

In order to better understand the role of NRP and *FyPP3* as a module in balancing growth and abiotic stress adaptation, global gene expression analysis was done with RNA sequencing (RNA-Seq). Six-day-old seedlings of four genotypes – WT, *nrp1 nrp2*, *FyPP3DN* and *nrp1 nrp2 FyPP3DN* – with or without 24 h of ABA treatment were compared. The general information on the RNA-Seq data is summarized in Materials and Methods.

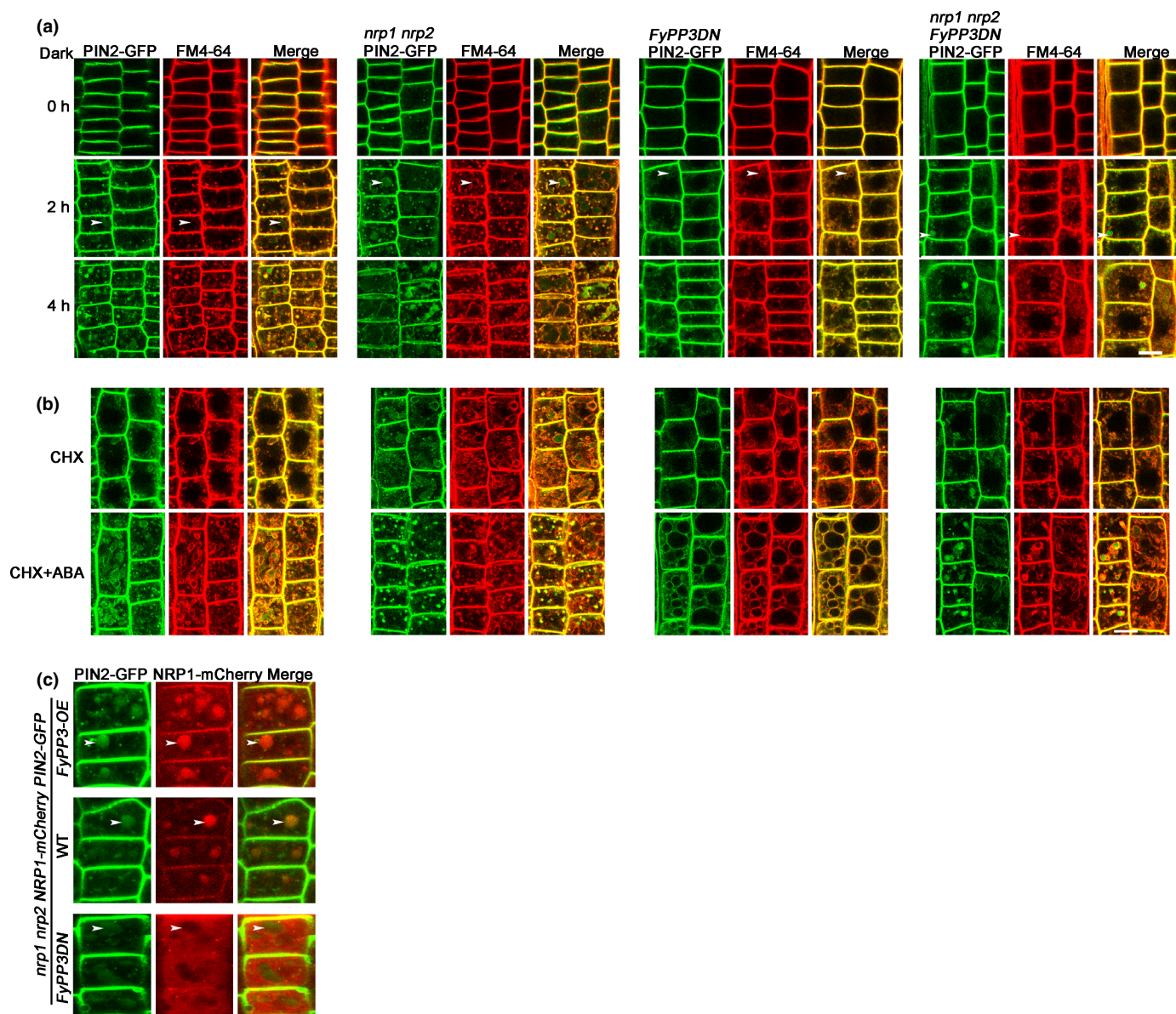


Fig. 6 Asparagine Rich Protein (NRP) and phytochrome-associated serine/threonine protein phosphatase 3 (FyPP3) act antagonistically on PIN-FORMED (PIN)2 vacuolar degradation. (a) Laser scanning confocal microscopy (LSCM) of PIN2-GFP in 5-d-old Arabidopsis wild-type (WT), *nrp1 nrp2*, *FyPP3DN* and *nrp1 nrp2 FyPP3DN* seedlings, before (0 h) and after dark treatment. Pulse-chase labeling with FM4-64 revealed that the dark-induced vacuolar degradation of PIN2 was the fastest in *nrp1 nrp2* and the slowest in *FyPP3DN*. Arrowheads indicate co-localization. (b) 5-d-old seedlings in (a) were treated with dark plus CHX (50 μ M) for 4 h, or with dark plus CHX for 3 h, then with dark plus CHX and abscisic acid (ABA) (100 μ M) for 1 h. ABA promoted vacuolar accumulation of PIN2 in both the WT and *nrp1 nrp2 FyPP3DN*, but not in *nrp1 nrp2* or *FyPP3DN*. (c) Effect of FyPP3 over-expression (*FyPP3-OE*) and loss-of-function (*FyPP3DN*) on ABA/dark-induced NRP1 and PIN2 subcellular distribution. The *FyPP3* constructs were introduced into *nrp1 nrp2 NRP1-mCherry PIN2-GFP* lines, and the seedlings were treated with ABA (100 μ M)/dark for 1 h. ABA promoted co-localization of NRP1 and PIN2 in the vacuole, and the co-localization was FyPP3-dependent. Arrowheads indicate co-localization. Bars: (a–c) 10 μ m.

Expression of 32 833 TAIR 10 gene models were detected, and 19 744 genes had an average Reads Per Kilobase per Million mapped reads (RPKM) larger than 0.5, and are thus considered as expressed. 14 131 genes passed the stable expression test with their $SD \leq \text{Mean}$, and the Venn diagrams illustrated the numbers of up- and downregulated genes by at least two folds (Log_2 fold change > 1) with or without ABA (Fig. 7a). Both principal component analysis (PCA) and hierarchical clustering over stably expressed genes showed that *FyPP3DN* was relatively different

from other genotypes in gene expression, either with or without ABA, and that knock-out of *NRP3* largely restored these shifts in gene expression (Figs S12, 7b). Genes in each cluster (cg) are listed in Table S2. To better describe the impact of NRP and FyPP3 on ABA- and auxin-mediated processes, we manually generated two gene lists, covering biosynthesis, metabolism, transport and signaling of auxin and ABA (Fig. S13A–D; Tables S3, S4). Hierarchical clustering on the 82 auxin-related genes showed that *nrp1 nrp2* and the WT were most similar in their expression

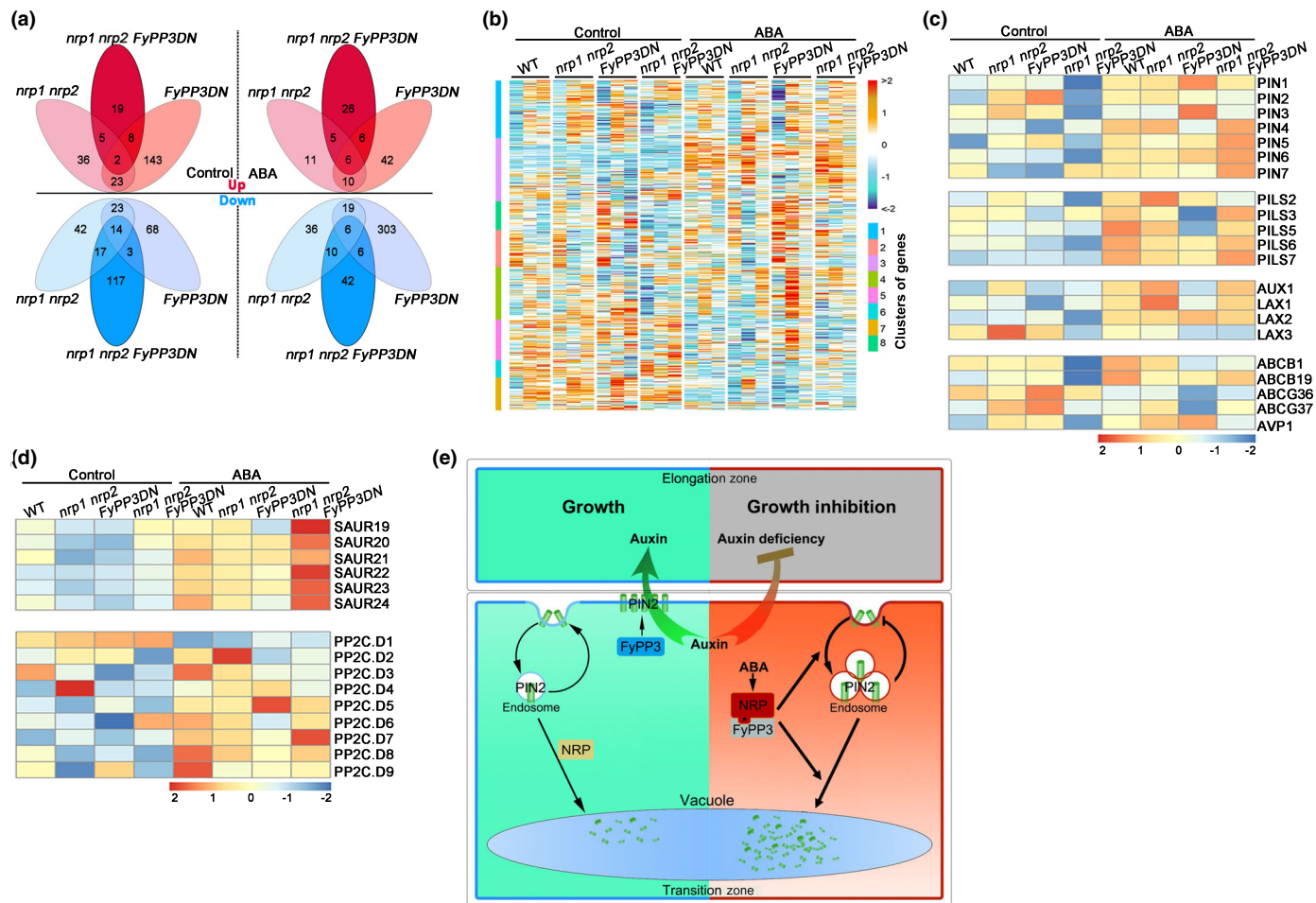


Fig. 7 RNA sequencing analyses reveal a critical role of Arginine Rich Protein–phytochrome-associated serine/threonine protein phosphatase 3 (NRP–FyPP3) module in abscisic acid (ABA)–auxin crosstalk. (a) Venn diagram showing the overlap in the number of transcripts up- and downregulated by two-fold relative to the wild-type (WT) in *nrp1 nrp2*, *FyPP3DN* and *nrp1 nrp2 FyPP3DN* with or without ABA. (b) Heat map showing the count per million (CPM) value of 14 131 genes that passed the stable expression test in four genotypes with or without ABA. The CPM value for each gene was calculated relative to the centralized matrix. Color bar of gene-clusters is shown and gene tables of the clusters given in Supporting Information Table S2. (c) Heat map showing the expression of selected auxin transport genes. (d) Heat map showing the expression of *SAUR19-24* subfamily of *SMALL AUXIN UP-RNAs* (*SAURs*) and the *PP2C.D* genes. (e) A working model. In the growth condition (left), in the transition zone, NRP is required for PIN2 vacuolar degradation. FyPP3, as a protein phosphatase, promotes basal plasma membrane (PM) localization of PIN2. Both proteins are required for establishing PIN2 polarity, and subsequently, for the basipetal auxin transport and the formation of the elongation zone. When stressed (right), ABA induces NRP expression. NRP recruits FyPP3, gets dephosphorylated by FyPP3, and further promotes vacuolar degradation of a subpopulation of PIN2 which without ABA would recycle back to the PM. ABA, which promotes PIN2 vacuolar degradation in an NRP-dependent way, thus condensing auxin at the root meristem and inhibiting auxin flux into the elongation zone to suppress primary root growth.

patterns, followed by *nrp1 nrp2 FyPP3DN*. *FyPP3DN* was very different in auxin-related gene expression either with or without ABA (Fig. S13A). The heat map generally was consistent with the phenotypes observed: the *nrp1 nrp2* double mutant had normal auxin response, the *nrp1 nrp2 FyPP3DN* lines looked like the WT, and FyPP3 has impacts on multiple signaling events.

The auxin transport genes gave more interesting details (Fig. 7c). *nrp1 nrp2 FyPP3DN* generally had much lower expression in genes involved in polar auxin transport, indicative of a feedback to the loss of the NRP–FyPP3-mediated vacuolar degradation pathway. Consistent with a genome-wide study on the soybean *PIN* gene family (Wang *et al.*, 2015), ABA treatment induced the expression of auxin transporters and carriers in several genotypes, likely resulting in over-accumulation of auxin and

growth retardation. Quantitative RT-PCR on *PIN* genes was more or less consistent with these observations, except for *FyPP3DN*, in which ABA-induced *PIN1* and *PIN2* expression and ABA-repressed *PIN3/4/6/7* expression was observed (Fig. S13E). To see if such an expression pattern is specific for auxin transporters and carriers, or rather a general pattern for PM-localized transporters, we looked at the expression of 45 P-type ATPases for a comparison (Axelsen & Palmgren, 2001) (Fig. S14A,B). These ion pumps appeared to be regulated very differently by ABA and no such consistent expression pattern was seen (Fig. S14A). Even if we looked closer at *AHA1-11* only (the PM proton pump subfamily, important for auxin-induced cell expansion), these genes still displayed individual and distinct expression patterns (Fig. S14B). The comparison suggested that

the expression of auxin transporters and carriers likely are specifically affected by the loss of NRP and FyPP3, and that ABA can over-rule such downregulation.

SMALL AUXIN UP-RNA (SAURs) were among the earliest genes to be identified as auxin-responsive (Franco *et al.*, 1990). Among all *SAURs*, the *SAUR19–24* subfamily emerged as most strikingly and uniformly regulated in our experiment (Figs S15, 7d). These essential players in auxin-mediated cell elongation and tropism are known to interact with and to antagonize the function of the PM-localized PP2C.D family phosphatases, thus freeing the PM proton pumps to promote acid growth (Spartz *et al.*, 2014; Ren *et al.*, 2018; Wang *et al.*, 2020). These *SAURs* were mostly repressed in *nrp1 nrp2* and *FyPP3DN* (Fig. 7d), consistent with the dwarf phenotype observed in either genotype. Like the auxin carriers, their transcription was strongly induced by ABA treatment. The PP2C.Ds also exhibited similar expression profiles (Fig. 7d). The consistent expression patterns observed in the auxin carriers and transporters, *SAUR19* family members, and PP2C.Ds indicated that the NRP-FyPP3 module specifically regulates auxin-mediated seedling growth and is required in ABA-induced growth suppression. We summarized the functions of NRP and FyPP3 in a model (Fig. 7e). FyPP3 and NRP not only work as a module in regulating ABI5-induced gene expression (Zhu *et al.*, 2018), but are critical in either polar PM distribution (FyPP3) or vacuolar degradation (NRP) of PIN. The two regulatory roles are connected by ABA, which promotes PIN2 vacuolar degradation in an NRP-dependent way, thus condensing auxin at the root meristem and inhibiting auxin flux into the elongation zone to suppress primary root growth.

Discussion

In this study, we uncovered an unexpected role in maintaining primary root elongation for the stress responsive proteins Asparagine Rich Protein (NRP)1 and NRP2. Such a function is partially achieved by promoting the constitutive vacuolar turnover of PIN-FORMED (PIN)2, the key auxin efflux carrier in the establishment of root elongation zone, and hence primary root elongation. We also showed that the abiotic stress hormone ABA can not only promote endocytosis, but also direct an exocytosis pool of PIN2 to the vacuole for degradation. NRP is required in both processes, as PIN2-GFP in *nrp1 nrp2* became significantly less sensitive to ABA treatment (GFP, green fluorescent protein). Therefore, NRP not only acts as a positive regulator in ABA signaling by stabilizing ABSCISIC ACID INSENSITIVE 5 (ABI5) (Zhu *et al.*, 2018), but also act as a switch in ABA-elicited trafficking route shunt. In other words, ABA employs NRP in both a signaling and a trafficking pathway to suppress plant growth.

We also discovered an important role for phytochrome-associated serine/threonine protein phosphatase 3 (FyPP3) in NRP-mediated PIN2 turnover. Suppressing FyPP3 function in *nrp1 nrp2* alleviated the dwarf phenotype of *nrp1 nrp2*, with the subcellular localization pattern of PIN2 and the auxin distribution in the meristematic and elongation zones (MZ and EZ) both

restored. The sensitivity to ABA in PIN2 vacuolar degradation is also restored in *nrp1 nrp2 FyPP3DN*. Importantly, the mutual vacuolar degradation of PIN2 and NRP is regulated by FyPP3. Over-expression of FyPP3 promotes accumulation of PIN2 and NRP1 in the vacuole, and suppressing FyPP3 activity prevented PIN2 and NRP1 from getting into the vacuole. These observation were consistent with our previous finding that de-phosphorylation of NRP by FyPP3 is required for mutual vacuolar degradation of FyPP3 and NRP, which is triggered by ABA. Finally, FyPP3 may have an additional function in positively regulating the endosomal sorting complexes required for transport (ESCRT) machinery: in *FyPP3DN*, ABA can induce PIN2 endocytosis; however, PIN2 accumulated at the tonoplast instead of getting into the vacuole, which is typically observed in the ESCRT mutants.

The interplay of phytohormones is usually intriguingly complex, often involving positive and negative regulators competing for a shared set of downstream machinery. In this particular case, ABA and auxin both regulate the amount, and subcellular and polar PM distribution of PIN2. ABA could inhibit PIN2-directed shootward auxin transport in at least two ways that involve NRP. First, FyPP3 is tethered by NRP for vacuolar degradation, leading to the stabilization and activation of the transcription factor ABI5 (Zhu *et al.*, 2018). ABI5 had been shown to repress PIN1 protein accumulation, thus reducing auxin concentration at the root meristem (Yuan *et al.*, 2014). Insufficient auxin at the meristematic zone could lead to insufficient auxin transport into the elongation zone. Second, ABA promotes PIN2 vacuolar degradation in an NRP-dependent way, preventing a subpopulation of endosomal PIN2 from recycling back to the plasma membrane (PM). Either way, the basipetal transport of auxin into the elongation zone and the subsequent root elongation is inhibited. As reported, ABA also induced transcription of auxin transport genes, as well as *SMALL AUXIN UP-RNA (SAUR)19–24* and PP2C.D phosphatases. These findings are in line with previous knowledge that auxin functions downstream of ABA in nearly all known interactions, and that auxin transport, especially its efflux, is regulated by ABA in suppressing germination and seedling growth (Emenecker & Strader, 2020), and could be one explanation for how the ABA–auxin interaction occurs.

The complexity of ABA and auxin signaling also is reflected in the way that multiple kinases, phosphatases and adaptor proteins regulate similar signaling events, and that vacuolar degradation of the signaling components often is involved. So far, PIN phosphorylation and de-phosphorylation had been reported to be conducted by PINOID (PID) and D6PKs, MAP kinases (MAPKs), and PP2A and PP6 protein phosphatases. Without stress, the PYRABACTIN RESISTANCE1-LIKE (PYL)/REGULATORY COMPONENTS OF ABA RECEPTORS (RCAR) ABA receptors can be phosphorylated by the Target of Rapamycin (TOR) kinase, and thus stay disassociated from PP2Cs and ABA. ABA-activated SNF1-related protein kinase 2 (SnRK2s) in turn phosphorylate Raptor, an adaptor for TOR, thus disassembling the TOR complex and releasing PYL from inhibition (Wang *et al.*, 2018). The PYL/RCAR receptors themselves are START domain

containing scaffold proteins that can be considered as inhibitory adaptors for PP2Cs. Furthermore, upon ABA induction, ubiquitinated PYLs can be tethered by FYVE1/FREE1, an ESCRT component (Gao *et al.*, 2014), for vacuolar degradation (Belda-Palazon *et al.*, 2016). ABA also can trigger FREE1 phosphorylation by SnRK2 to induce FREE1 nuclear import, leading to its interaction with ABI5 and ABF4 and suppression of ABA signaling (Li *et al.*, 2019). Recently, the PYLs–PP2A complex has been established as a new module that balances root growth and stress adaptation (Li *et al.*, 2020). Without stress, PYLs interact with PP2A to antagonize PID-mediated PIN phosphorylation. Upon stress, ABA binds to PYLs to inhibit PP2A activity, leading to PIN phosphorylation and inhibition of basipetal transport of auxin in the root. Our observations on NRP, the (likely) scaffold, and FyPP3 (PP6), the phosphatase, brings another scaffold–phosphatase module to the menu. This module differs from others in two ways. First, NRP itself acts as a trafficking regulator, rather than a substrate for degradation. Second, FyPP3, or PP6, is an ancient protein phosphatase coded by only two genes in Arabidopsis, and it carries multiple essential functions. We postulated that this very simple module likely only forms in emergencies, and could be one of the earliest growth-to-survival strategies for land plants.




Acknowledgements

We thank Mingqiu Dai, Shuzhen Men and Ben Scheres for sharing published materials; Jiuzhi Qi, Daqi Yu and Yong Zhang for suggestions on RNA-seq analysis; and Shisong Ma and Yang Zhao for critical readings of the manuscript. The authors declare no conflicts of interest. This work is supported by the National Key Research and Development Program of China (2017YFD0200900) to XL, the National Natural Science Foundation of China (91954102 and 31871355 to QG, 31870730 to XL), and Tianjin Natural Science Foundation (17JCZDJC31900 to XL, 18JCZDJC32300 to QG).

Author contributions

XL and QG, conceptualization; XL and QG, methodology; YW, YC, WT, investigation; LL, software and data curation; YW, LL, XL and QG, writing – original draft; QG, writing – review & editing; XL and QG, funding acquisition; and XL and QG, supervision.

ORCID

Qingqiu Gong  <https://orcid.org/0000-0002-9803-8554>
Xinqi Liu  <https://orcid.org/0000-0002-6045-718X>
Yanying Wu  <https://orcid.org/0000-0002-6682-3451>

Data availability

The RNA-sequencing data have been deposited to the Gene Expression Omnibus (GEO) under the accession number GSE150648.

References

- Alves MS, Reis PA, Dadalto SP, Faria JA, Fontes EP, Fietto LG. 2011. A novel transcription factor, ERD15 (Early Responsive to Dehydration 15), connects endoplasmic reticulum stress with an osmotic stress-induced cell death signal. *Journal of Biological Chemistry* **286**: 20020–20030.
- Axelsen KB, Palmgren MG. 2001. Inventory of the superfamily of P-type ion pumps in Arabidopsis. *Plant Physiology* **126**: 696–706.
- Bailey-Serres J, Parker JE, Ainsworth EA, Oldroyd GED, Schroeder JJ. 2019. Genetic strategies for improving crop yields. *Nature* **575**: 109–118.
- Barbosa IC, Zourelidou M, Willige BC, Weller B, Schwechheimer C. 2014. D6 PROTEIN KINASE activates auxin transport-dependent growth and PIN-FORMED phosphorylation at the plasma membrane. *Development Cell* **29**: 674–685.
- Belda-Palazon B, Rodriguez L, Fernandez MA, Castillo M-C, Anderson EM, Gao C, Gonzalez-Guzman M, Peirats-Llobet M, Zhao Q, De Winne N *et al.* 2016. FYVE1/FREE1 interacts with the PYL4 ABA receptor and mediates its delivery to the vacuolar degradation pathway. *Plant Cell* **28**: 2291–2311.
- Belin C, Megies C, Hauserova E, Lopez-Molina L. 2009. Absciscic acid represses growth of the Arabidopsis embryonic axis after germination by enhancing auxin signaling. *Plant Cell* **21**: 2253–2268.
- Benkova E, Michniewicz M, Sauer M, Teichmann T, Seifertova D, Jurgens G, Friml J. 2003. Local, efflux-dependent auxin gradients as a common module for plant organ formation. *Cell* **115**: 591–602.
- de Camargos LF, Fraga OT, Oliveira CC, da Silva JCF, Fontes EPB, Reis PAB. 2018. Development and cell death domain-containing asparagine-rich protein (DCD/NRP): an essential protein in plant development and stress responses. *Theoretical and Experimental Plant Physiology* **31**: 59–70.
- Dai M, Terzaghi W, Wang H. 2013a. Multifaceted roles of Arabidopsis PP6 phosphatase in regulating cellular signaling and plant development. *Plant Signaling & Behavior* **8**: e22508.
- Dai M, Xue Q, McCray T, Margavage K, Chen F, Lee JH, Nezames CD, Guo L, Terzaghi W, Wan J *et al.* 2013b. The PP6 phosphatase regulates ABI5 phosphorylation and abscisic acid signaling in Arabidopsis. *Plant Cell* **25**: 517–534.
- Dai M, Zhang C, Kania U, Chen F, Xue Q, McCray T, Li G, Qin G, Wakeley M, Terzaghi W *et al.* 2012. A PP6-type phosphatase holoenzyme directly regulates PIN phosphorylation and auxin efflux in Arabidopsis. *Plant Cell* **24**: 2497–2514.
- Dhonukshe P, Aniento F, Hwang I, Robinson DG, Mravec J, Stierhof YD, Friml J. 2007. Clathrin-mediated constitutive endocytosis of PIN auxin efflux carriers in Arabidopsis. *Current Biology* **17**: 520–527.
- Ebine K, Okatani Y, Uemura T, Goh T, Shoda K, Niihama M, Morita MT, Spitzer C, Otegui MS, Nakano A *et al.* 2008. A SNARE complex unique to seed plants is required for protein storage vacuole biogenesis and seed development of *Arabidopsis thaliana*. *Plant Cell* **20**: 3006–3021.
- Emenecker RJ, Strader LC. 2020. Auxin-abscisic acid interactions in plant growth and development. *Biomolecules* **10**: 281.
- Franco AR, Gee MA, Guilfoyle TJ. 1990. Induction and superinduction of auxin-responsive mRNAs with auxin and protein synthesis inhibitors. *Journal of Biological Chemistry* **265**: 15845–15849.
- Friml J, Yang X, Michniewicz M, Weijers D, Quint A, Tietz O, Benjamins R, Ouwerkerk PB, Jung K, Sandberg G *et al.* 2004. A PINOID-dependent binary switch in apical-basal PIN polar targeting directs auxin efflux. *Science* **306**: 862–865.
- Galvan-Ampudia CS, Julkowska MM, Darwish E, Gandullo J, Korver RA, Brunoud G, Haring MA, Munnik T, Vernoux T, Testerink C. 2013. Halotropism is a response of plant roots to avoid a saline environment. *Current Biology* **23**: 2044–2050.
- Gao C, Luo M, Zhao Q, Yang R, Cui Y, Zeng Y, Xia J, Jiang L. 2014. A unique plant ESCRT component, FREE1, regulates multivesicular body protein sorting and plant growth. *Current Biology* **24**: 2556–2563.
- Geldner N, Friml J, Stierhof YD, Jurgens G, Palme K. 2001. Auxin transport inhibitors block PIN1 cycling and vesicle trafficking. *Nature* **413**: 425–428.
- Gong Z, Xiong L, Shi H, Yang S, Herrera-Estrella LR, Xu G, Chao D-Y, Li J, Wang P-Y, Qin F *et al.* 2020. Plant abiotic stress response and nutrient use efficiency. *Science China-Life Sciences* **063**: 635–674.

- Guo X, Qin Q, Yan J, Niu Y, Huang B, Guan L, Li Y, Ren D, Li J, Hou S. 2015. TYPE-ONE PROTEIN PHOSPHATASE4 regulates pavement cell interdigitation by modulating PIN-FORMED1 polarity and trafficking in Arabidopsis. *Plant Physiology* 167: 1058–1075.
- He W, Brumos J, Li H, Ji Y, Ke M, Gong X, Zeng Q, Li W, Zhang X, An F *et al.* 2011. A small-molecule screen identifies L-kynurenine as a competitive inhibitor of TAA1/TAR activity in ethylene-directed auxin biosynthesis and root growth in Arabidopsis. *Plant Cell* 23: 3944–3960.
- Heisler MG, Ohno C, Das P, Sieber P, Reddy GV, Long JA, Meyerowitz EM. 2005. Patterns of auxin transport and gene expression during primordium development revealed by live imaging of the Arabidopsis inflorescence meristem. *Current Biology* 15: 1899–1911.
- Jia W, Li B, Li S, Liang Y, Wu X, Ma M, Wang J, Gao J, Cai Y, Zhang Y *et al.* 2016. Mitogen-activated protein kinase cascade MKK7-MPK6 plays important roles in plant development and regulates shoot branching by phosphorylating PIN1 in Arabidopsis. *PLoS Biology* 14: e1002550.
- Kakei Y, Yamazaki C, Suzuki M, Nakamura A, Sato A, Ishida Y, Kikuchi R, Higashi S, Kokudo Y, Ishii T *et al.* 2015. Small-molecule auxin inhibitors that target YUCCA are powerful tools for studying auxin function. *The Plant Journal* 84: 827–837.
- Karampelias M, Neyt P, De Groeve S, Aesaert S, Coussens G, Rolcik J, Bruno L, De Winne N, Van Minnebruggen A, Van Montagu M *et al.* 2016. ROTUNDA3 function in plant development by phosphatase 2A-mediated regulation of auxin transporter recycling. *Proceedings of the National Academy of Sciences, USA* 113: 2768–2773.
- Kim DH, Kang JG, Yang SS, Chung KS, Song PS, Park CM. 2002. A phytochrome-associated protein phosphatase 2A modulates light signals in flowering time control in Arabidopsis. *Plant Cell* 14: 3043–3056.
- Kleine-Vehn J, Ding Z, Jones AR, Tasaka M, Morita MT, Friml J. 2010. Gravity-induced PIN transcytosis for polarization of auxin fluxes in gravity-sensing root cells. *Proceedings of the National Academy of Sciences, USA* 107: 22344–22349.
- Kleine-Vehn J, Leitner J, Zwiewka M, Sauer M, Abas L, Luschnic G, Friml J. 2008. Differential degradation of PIN2 auxin efflux carrier by retromer-dependent vacuolar targeting. *Proceedings of the National Academy of Sciences, USA* 105: 17812–17817.
- Li H, Li Y, Zhao Q, Li T, Wei J, Li B, Shen W, Yang C, Zeng Y, Rodriguez PL *et al.* 2019. The plant ESCRT component FREE1 shuttles to the nucleus to attenuate abscisic acid signalling. *Nature Plants* 5: 512–524.
- Li H, Lin D, Dhonukshe P, Nagawa S, Chen D, Friml J, Scheres B, Guo H, Yang Z. 2011. Phosphorylation switch modulates the interdigitated pattern of PIN1 localization and cell expansion in Arabidopsis leaf epidermis. *Cell Research* 21: 970–978.
- Li Y, Wang Y, Tan S, Li Z, Yuan Z, Glanc M, Domjan D, Wang K, Xuan W, Guo Y *et al.* 2020. Root growth adaptation is mediated by PYLs ABA receptor-PP2A protein phosphatase complex. *Advanced Science* 7: 1901455.
- Lillo C, Kataya AR, Heidari B, Creighton MT, Nemie-Feyissa D, Ginbot Z, Jonassen EM. 2014. Protein phosphatases PP2A, PP4 and PP6: mediators and regulators in development and responses to environmental cues. *Plant, Cell & Environment* 37: 2631–2648.
- Michniewicz M, Zago MK, Abas L, Weijers D, Schweighofer A, Meskiene I, Heisler MG, Ohno C, Zhang J, Huang F *et al.* 2007. Antagonistic regulation of PIN phosphorylation by PP2A and PINOID directs auxin flux. *Cell* 130: 1044–1056.
- Petrasek J, Mravec J, Bouchard R, Blakeslee JJ, Abas M, Seifertova D, Wisniewska J, Tadele Z, Kubes M, Covanova M *et al.* 2006. PIN proteins perform a rate-limiting function in cellular auxin efflux. *Science* 312: 914–918.
- Reis PAB, Carpinetti PA, Freitas PPJ, Santos EGD, Camargos LF, Oliveira IHT, Silva JCF, Carvalho HH, Dal-Bianco M, Soares-Ramos JRL *et al.* 2016. Functional and regulatory conservation of the soybean ER stress-induced DCD/NRP-mediated cell death signaling in plants. *BMC Plant Biology* 16: 156.
- Reis PA, Rosado GL, Silva LA, Oliveira LC, Oliveira LB, Costa MD, Alvim FC, Fontes EP. 2011. The binding protein BiP attenuates stress-induced cell death in soybean via modulation of the N-rich protein-mediated signaling pathway. *Plant Physiology* 157: 1853–1865.
- Ren H, Park MY, Spartz AK, Wong JH, Gray WM. 2018. A subset of plasma membrane-localized PP2C.D phosphatases negatively regulate SAUR-mediated cell expansion in Arabidopsis. *PLoS Genetics* 14: e1007455.
- Rowe JH, Topping JF, Liu J, Lindsey K. 2016. Abscisic acid regulates root growth under osmotic stress conditions via an interacting hormonal network with cytokinin, ethylene and auxin. *New Phytologist* 211: 225–239.
- Shimizu Y, Takagi J, Ito E, Ito Y, Ebine K, Komatsu Y, Goto Y, Sato M, Toyooka K, Ueda T *et al.* 2021. Cargo sorting zones in the trans-Golgi network visualized by super-resolution confocal live imaging microscopy in plants. *Nature Communication* 12: 1901.
- Spartz AK, Ren H, Park MY, Grandt KN, Lee SH, Murphy AS, Sussman MR, Overvoorde PJ, Gray WM. 2014. SAUR inhibition of PP2C-D phosphatases activates plasma membrane H⁺-ATPases to promote cell expansion in Arabidopsis. *Plant Cell* 26: 2129–2142.
- Spitzer C, Reyes FC, Buono R, Sliwinski MK, Haas TJ, Otegui MS. 2009. The ESCRT-related CHMP1A and B proteins mediate multivesicular body sorting of auxin carriers in Arabidopsis and are required for plant development. *Plant Cell* 21: 749–766.
- Swarup R, Friml J, Marchant A, Ljung K, Sandberg G, Palme K, Bennett M. 2001. Localization of the auxin permease AUX1 suggests two functionally distinct hormone transport pathways operate in the Arabidopsis root apex. *Genes Development* 15: 2648–2653.
- Tenhaken R, Doerks T, Bork P. 2005. DCD - a novel plant specific domain in proteins involved in development and programmed cell death. *BMC Bioinformatics* 6: 169.
- Uhrig RG, Labandera AM, Moorhead GB. 2013. Arabidopsis PPP family of serine/threonine protein phosphatases: many targets but few engines. *Trends in Plant Science* 18: 505–513.
- Wang P, Zhao Y, Li Z, Hsu C-C, Liu X, Fu L, Hou Y-J, Du Y, Xie S, Zhang C *et al.* 2018. Reciprocal regulation of the TOR kinase and ABA receptor balances plant growth and stress response. *Molecular Cell* 69: e106.
- Wang X, Yu R, Wang J, Lin Z, Han X, Deng Z, Fan L, He H, Deng XW, Chen H. 2020. The asymmetric expression of SAUR genes mediated by ARF7/19 promotes the gravitropism and phototropism of plant hypocotyls. *Cell Reports* 31: 107529.
- Wang Y, Chai C, Valliyodan B, Maupin C, Annen B, Nguyen HT. 2015. Genome-wide analysis and expression profiling of the PIN auxin transporter gene family in soybean (*Glycine max*). *BMC Genomics* 16: 951.
- Weller B, Zourelidou M, Frank L, Barbosa IC, Fastner A, Richter S, Jurgens G, Hammes UZ, Schwechheimer C. 2017. Dynamic PIN-FORMED auxin efflux carrier phosphorylation at the plasma membrane controls auxin efflux-dependent growth. *Advanced Science* 114: E887–E896.
- Xu J, Scheres B. 2005. Dissection of Arabidopsis ADP-RIBOSYLATION FACTOR 1 function in epidermal cell polarity. *Plant Cell* 17: 525–536.
- Yang Y, Liu X, Zhang W, Qian Q, Zhou L, Liu S, Li Y, Hou X. 2021. Stress response proteins NRP1 and NRP2 are pro-survival factors that inhibit cell death during ER stress. *Plant Physiology*. doi: 10.1093/plphys/kiab335.
- Yu X, Dong J, Deng Z, Jiang Y, Wu C, Qin X, Terzaghi W, Chen H, Dai M, Deng XW. 2019. Arabidopsis PP6 phosphatases dephosphorylate PIF proteins to repress photomorphogenesis. *Proceedings of the National Academy of Sciences, USA* 116: 20218–20225.
- Yuan TT, Xu HH, Zhang KX, Guo TT, Lu YT. 2014. Glucose inhibits root meristem growth via ABA INSENSITIVE 5, which represses PIN1 accumulation and auxin activity in Arabidopsis. *Plant, Cell & Environment* 37: 1338–1350.
- Zhou R, Zhu T, Han L, Liu M, Xu M, Liu Y, Han D, Qiu D, Gong Q, Liu X. 2017. The asparagine-rich protein NRP interacts with the Verticillium effector PevD1 and regulates the subcellular localization of cryptochrome 2. *Journal of Experimental Botany* 68: 3427–3440.
- Zhu T, Wu Y, Yang X, Chen W, Gong Q, Liu X. 2018. The asparagine-rich protein NRP facilitates the degradation of the PP6-type phosphatase FyPP3 to promote ABA response in Arabidopsis. *Molecular Plant* 11: 257–268.
- Zwiewka M, Nodzynski T, Robert S, Vanneste S, Friml J. 2015. Osmotic stress modulates the balance between exocytosis and clathrin-mediated endocytosis in *Arabidopsis thaliana*. *Molecular Plant* 8: 1175–1187.

Supporting Information

Additional Supporting Information may be found online in the Supporting Information section at the end of the article.

Fig. S1 Gene structures and semi-quantitative RT-PCR detection of the *nrp1 nrp2* double mutant.

Fig. S2 Phenotype of *nrp1 nrp2* plants and the complementation lines.

Fig. S3 *nrp1 nrp2* responded normally to auxin biosynthesis inhibitors L-Kyn and PPBo.

Fig. S4 Auxin response is normal in *nrp1 nrp2*.

Fig. S5 The root basipetal transport assay of *nrp1 nrp2* seedlings.

Fig. S6 A synthetic phenotype was observed in *nrp1 nrp2 pin1*.

Fig. S7 Imaging of PIN1-GFP in WT and *nrp1 nrp2* seedling roots with CHX and BFA treatment.

Fig. S8 Co-immunoprecipitation detection of PIN2 and NRP1 proteins.

Fig. S9 Imaging of PIN1-GFP in WT and *nrp1 nrp2* seedling roots with BFA, ABA, and ConA treatment.

Fig. S10 The impact of FyPP3 on co-immunoprecipitation detection of PIN2 and NRP1 proteins.

Fig. S11 Partial co-localization of NRP1, NRP2, FyPP3, and marker proteins upon ABA treatment.

Fig. S12 PCA of the WT, *nrp1 nrp2*, *FyPP3DN* and *nrp1 nrp2 FyPP3DN* for the transcriptome dataset.

Fig. S13 Heat map of auxin- and ABA-related genes.

Fig. S14 Transcript levels of P-type ion pumps/ATPases in WT, *nrp1 nrp2*, *FyPP3DN* and *nrp1 nrp2 FyPP3DN*, with or without ABA.

Fig. S15 Hierarchical clustering of SAURs.

Methods S1 Detailed descriptions of materials and methods.

Table S1 Primers used in this study.

Table S2 Hierarchical clustering of genes that passed the stable expression test.

Table S3 Hierarchical clustering of 82 auxin-related genes.

Table S4 Hierarchical clustering of 104 ABA-related genes.

Video S1 3D movies of *DR5rev:3×VENUS* in WT and *nrp1 nrp2* seedlings.

Please note: Wiley Blackwell are not responsible for the content or functionality of any Supporting Information supplied by the authors. Any queries (other than missing material) should be directed to the *New Phytologist* Central Office.